Metallaphotoredox catalysis with organic dyes

MetallaPhotoredox Catalysis with Organic Dyes

Andrea Gualandi, Michele Anselmi, Francesco Calogero, Simone Potenti, Elena Bassan, Paola Ceroni, and Pier Giorgio Cozzi

Org. Biomol. Chem., **2021**, *19*, 3527-3550.

https://doi.org/10.1039/D1OB00196E

MetallaPhotoredox Catalysis with Organic Dyes

Andrea Gualandi,*[a] Michele Anselmi,[a] Francesco Calogero,[a] Simone Potenti,[a,b] Elena Bassan,[a] Paola Ceroni,[a] and Pier Giorgio Cozzi*[a]

The use of organic dyes to promote organic reactions by photoredox catalysis is continuosly expanding, and was recently reviewed by Nicewicz. The synthesis of new dyes, their application in flow photoredox reactions, their use in stereoselective and multicomponent trasformations have considerably expanded the repertoir of application of organic dyes in photoredox mediated reactions. The minor costs of these dyes, their tailored synthesis and availability in combination with the development of new concepts and careful catalytic cycle design (made possible by the application of fine theoretical investigations and deep understanding) are guiding the widespread application of organic dyes in the metalla photoredox catalysis area. Developments, and recent applications of different metal catalyzed processes mediated by organic dyes, are covered by this review.

1. Introduction

In photosynthesis, Nature uses light to drive chemical endergonic reactions transforming light's energy into chemical energy. Recently, laboratories all around the world are taking advantage of light in order to promote new organic reactions. In the last decade, photocatalysis applied to organic reactions has become a widely investigated subject.[1] Even if photochemistry has been a deeply investigated area,[2,3] both from a theoretical[4] and a practical[5] point of view, photochemistry applied to organic reactions has been mainly limited to direct excitation of one of the reactants by UV light. The use of photosensitizers, capable of absorbing visible light and promoting photoinduced electron or energy transfer processes, determined a revolution in the field for two main reasons: (i) less expensive light sources, particularly LEDs, or even sunlight, can be employed; (ii) visible light excitation can be selectively absorbed by the photosensitizers, avoiding photodegradation reactions of the organic substrates. The guiding model for the use of a photosensitizer is related to the properties of its excited state in terms of energy, lifetime and redox properties. To date, metal complexes, such as Ru(II) and Ir(III) complexes are considered exceptional photosensitizers in photoredox catalysis thanks to their long excited-state lifetimes and higher chemical stability of the oxidized and reduced forms.[6] However, ruthenium and iridium are rare and heavy elements. The use of photoredox catalysts based on Earth abundant metals[7] has attracted growing interest,[8] but still there are some drawbacks, such as supply (cobalt), efficiency (iron), and toxicity (nickel), that have limited their application in large-scale synthesis of active pharmaceutical ingredients (API).[9] The use of organic dyes as photosensitizers can overcome these drawbacks. Indeed, the diversity obtained by simple modification of known structures,[10] guided by theoretical tools,[11] offers potential solutions for the optimization of synthetic photoredox methodologies. In addition, there are advantages in employing organic dyes as photosensitizers related to their synthesis, scale-up, the absence of metals, and the possibility of selecting between many classes of organic compounds with a fine tuning of electronic and photophysical properties. A comprehensive and impressive review about organic molecules used as photosensitizers was recently reported by Nicewicz.[12] In the review collected by Nicewicz it is possible for the readers to address questions related to photophysical properties of the major classes of organic molecules employed in photoredox reactions. In 2011 a breakthrough was published by Sanford,[13] followed in 2014 by two key papers published by Doyle-MacMillan[14] and Molander,[15] exploiting the brilliant idea to use photoredox catalysis in metal-mediated processes.[16] The studies were carried out with iridium complex based photosensitizers. From the initial studies involving nickel catalysis[17] many metals, such as copper,[18] gold,[19] palladium,[20] rhodium,[21] ruthenium,[22] iron,[23] titanium[24] were employed in synergistic combination with metal photosensitizers in innovative catalytic processes. However, soon, the use of organic dyes started to be investigated to replace the expensive ruthenium and iridium photosensitizers, for more sustainable applications and methodologies. Since the synergistic metal catalysis with organic dyes has reached nowadays a high level of complexity and broad application, in this review we present the most salient results in this field. We have summarized the work done selecting a particular class of dyes, presenting different metal mediated processes, shedding light on the mechanistic understanding, the reaction investigated, and the results obtained.

2. General consideration for metallaphotocatalysis with organic dyes

Starting from the earliest developments of organic photoredox catalysis, several classes of organic dyes have been used to promote light-mediated processes. To date, it is possible to find several examples in literature involving cyanoarenes, flavins, xanthenes, thiazines, and many other derivatives.[12] However, only a limited number of them has been merged to metal catalysts for metallaphotocatalysis.

Organic dyes are usually characterized by closed-shell ground electronic configuration, so that the ground state has a singlet spin multiplicity (S_0), and the excited states are either singlets (S_1, S_2, etc.) or triplets (T_1, T_2, etc.) (see a representative Jablonski diagram in **Figure 1**).

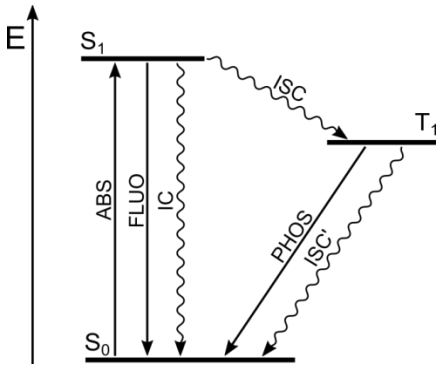

Figure 1 Jablonski diagram for organic molecules with radiative (straight lines) and non-radiative processes (wavy lines).

Absorption (ABS) bands correspond to electronic transitions between states of the same spin multiplicity, i.e. S_0-S_n transitions. The lowest-energy triplet excited state (T_1) can be populated by a non-radiative process, named intersystem crossing (ISC) from the S_1 excited state. This ISC process is expected to be efficient when a) heavy atoms are present;[26] b) the energy difference between the involved electronic states is low; c) the configuration of electronic states involved is different (El-Sayed rules). The excited state lifetime (τ) of the organic dye represents a crucial parameter when a bimolecular quenching process takes place in the photocatalytic cycle. Lifetime (τ) of excited states can vary from 10^{-10}–10^{-8} s for S_1 to 10^{-6}–10^{-3} s for T_1 in fluid solution. The quenching constant can be evaluated by the Stern-Volmer plot, measuring the lifetime of the photoreactive excited state of the photocatalyst as a function of the quencher concentration.[2, 3]

Most of the metallaphotocatalysis processes are based on photoinduced electron transfer reactions and are thus named metallaphotoredox catalysis. The electronically excited states are better oxidant and better reductant compared to the ground state species. Therefore, electron transfer reactions that are endoergonic in the dark become exoergonic upon light excitation of the organic photosensitizer (PS). The photoinduced electron transfer reactions are always single electron transfer processes, and the redox potentials of excited states can be evaluated according to the following equations:

$$E^0(PS^{\bullet+}/{}^*PS) = E^0(PS^{\bullet+}/PS) - [E_{00}({}^*PS/PS)/F] \qquad (1)$$
$$E^0({}^*PS/PS^{\bullet-}) = E^0(PS/PS^{\bullet-}) + [E_{00}({}^*PS/PS)/F] \qquad (2)$$

where E_{00}(*PS/PS) is the electronic energy of the excited state (i.e., the difference between the zero vibrational levels of ground and excited state) and F is the Faraday constant. It should be noted that E_{00}(*PS/PS) concerns the *reactive* excited state, which does not always coincide with the excited state directly populated by light absorption, e.g., in the case of photoreactive T_1 excited states.

It is important to underline that these equations are valid only for *reversible electron transfer processes*. When the electron transfer process is coupled to a chemical reaction, the evaluation of the thermodynamics is much more complicated.

The yields of the desired organic reactions are influenced not only by the efficiency of the electron transfer (eT) step, but also by the stability of the generated radical species and the kinetics of competitive reactions. Moreover, when designing a photoredox reaction, it is important to remember that, after photoinduced electron transfer, the photosensitizer needs to be restored to its initial oxidation state before starting a new catalytic cycle. This can be done by a sacrificial reagent or by an organic substrate, provided they have the proper redox potentials (Figure 2, A). For the sake of comparison, all the redox potentials need to be referred to the same standard electrode, e.g., standard calomel electrode (SCE).

An alternative mechanism to photoinduced electron transfer is energy transfer from the photosensitizer to the metal-based catalyst (Figure 2, B).[25] The rate of energy transfer is dependent on different parameters correlated to Coulombic or exchange mechanism,[2,3] but, in all cases, it is required that the excited state of the photosensitizer lies at higher energy than the excited state of the metal-based catalyst to be populated.

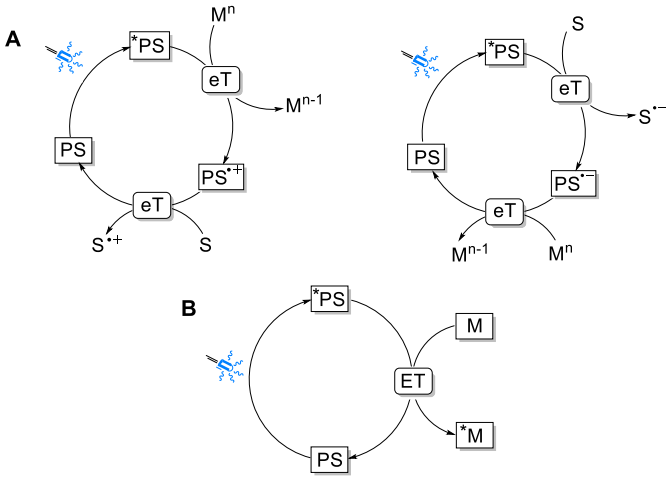

Figure 2 Examples of possible catalytic cycles involving photoinduced electron transfer processes (A). Catalytic cycle involving an energy transfer process (B). PS= photosensitizer; M= metal-based catalyst; S= sacrificial reagent or organic substrate; eT= electron transfer; ET= energy transfer.

3. Principal classes of organic dyes employed in metallaphotocatalysis and their properties

In this section the fundamental photophysical and electrochemical properties of organic dyes, which are most commonly used in metallaphotocatalysis, are discussed. The redox potential values are reported vs. SCE.

3.1 Cyanobenzene derivatives

Dicyanobenzene derivatives were first reported by Adachi in 2012 as novel materials for light-emitting diodes (OLEDs)[26]. These dyes are characterized by a thermally activated delayed fluorescence (TADF) as a result of the very small energy gap between their singlet and triplet excited states. In fact, when the S_1-T_1 splitting is small (ΔE ca. 100 meV for this class of molecules), reverse intersystem crossing from T_1 to S_1 is possible at room temperature. The triplet state is long-lived and delayed fluorescence follows the triplet state population. The molecular design of dicyanobenzene derivatives is critical to have both a small S_1-T_1 energy splitting and a high fluorescence decay rate. The latter property is highly desired in OLED materials, since it ensures a high luminescence quantum yield, but is not strictly necessary in photoredox catalysis. In order to fulfill the above-mentioned criteria for the realization of a molecule presenting TADF, the highest occupied molecular orbital (HOMO) and the lowest unoccupied molecular orbital (LUMO) of these dyes must be localized on the donor and acceptor moieties, respectively, leading to a charge transfer transition characterized by small $\Delta E_{S1\text{-}T1}$. This goal has been reached, for example, by coupling electron donating carbazolyl units to an electron accepting dicyanobenzene unit. In the case of **4CzIPN** (2,4,5,6-tetra(9H-carbazol-9-yl)isophthalonitrile (**PS-I**, Figure 3), it is possible to populate its lowest excited state by irradiation with blue light (absorbance onset in MeCN at 470 nm and molar absorption coefficient of ca. 20000 $M^{-1}cm^{-1}$ at 375 nm) and an emission can be detected at 539 nm.[27] This emission has a monoexponential decay in aerated solutions (τ = 12.7 ns in MeCN, prompt fluorescence[27]) but shows a biexponential decay in degassed solutions. The second mentioned decay occurs in the range of microseconds and depends on the concentration of molecular oxygen and temperature, as is typical of delayed fluorescence. Thanks to the localized nature of the HOMO and LUMO orbitals, the electrochemical properties of this class of dyes are strongly dependent on those of the parent electron donating and electron accepting units. Moreover, one advantage of the use of TADF-displaying dyes is that the E_{00} used to determine the excited state redox potentials is that of the singlet state, and therefore the loss of excitation energy is minimized. For example, for **PS-I** $E(PS^{\bullet+}/PS)$ is +1.49 V and $E(PS/PS^{\bullet-})$ is -1.24 V, and considering E_{00} = 2.67 eV, $E(PS^{\bullet+}/{}^*PS)$= -1.18 V and $E({}^*PS/PS^{\bullet-})$= +1.43 V (vs. SCE in MeCN).[27] A different dicyanobenzene derivative that has been used in metallaphotocatalysis is **3DPAFIPN** (2,4,6-tris(diphenylamino)-5-fluoroisophthalonitrile (**PS-II**, Figure 3). The photophysical properties of this dye are largely similar to those of **PS-I**. However, the presence of a halogen atom directly bonded to the core of the molecule and the presence of the better electron-donating diphenyl amino moiety instead of carbazole determine a lowering both for the reduction or the oxidation potentials.[27] By choosing the appropriate electron donating and electron accepting units, it is therefore possible to tune the redox potentials of dicyanobenzene derivatives to meet those requested from the desired reaction.

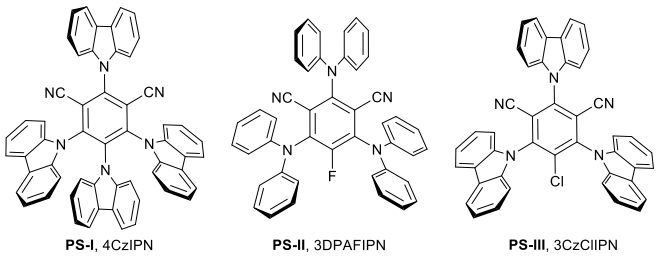

Figure 3. Dicyanobenzene-based photosensistizers.

3.2 Carbonyl compounds

Carbonyl compounds are a wide class of organic molecules that possess a double bond between a carbon and an oxygen atom. One of the most interesting features of this class of compounds is that the triplet state that arises from the $\pi \rightarrow \pi^*$ electronic transition can lie below or very close in energy to the singlet state that arises from the $n \rightarrow \pi^*$ transition. Thanks to El-Sayed rules,[3] intersystem crossing between these two states is very fast and the long-lived triplet excited state can be efficiently populated. In this context, the most representative example is **benzophenone** (**PS-IV**, Figure 4). Its absorption spectrum presents one weaker band at 350 nm, resulted from the symmetry-forbidden $n \rightarrow \pi^*$ transition, and a stronger one at 250 nm, derived from the allowed $\pi \rightarrow \pi^*$ transition. The emission spectrum is characterized by two bands, as well: the most intense one is the phosphorescence in the range of 400-550 nm and a weak tail on the high energy side is due to thermally activated delayed fluorescence. In a rigid matrix at 77K, the triplet state has a lifetime of 10^{-3} s.[28] The efficiency of the ISC is unitary with a quantum yield associated to the population of the triplet excited state of 100%.[3] The reduction potentials of carbonyl compounds are generally quite negative, which implies that, if reduced, these photosensitizers are good reductants: in the case of **PS-IV**, E(PS/PS$^{\bullet-}$) is -1.83 V vs. SCE in MeCN.[29]

Recently, a derivative of benzophenone bearing an electron withdrawing group on one phenyl ring and an electron donating one on the other one has been utilized as a photosensitizer.[30] This compound has a higher absorption at 350 nm but still suffers from the drawback of absorbing UV light exclusively. **Thioxanthone** (**PS-VII**, Figure 4) has also been utilized in metallaphotoredox catalysis.[31] Its molar absorption coefficient is significantly higher compared to that of **PS-IV** and its lowest absorption band is slightly red-shifted.[31] However, this sensitizer still fails at absorbing visible light.

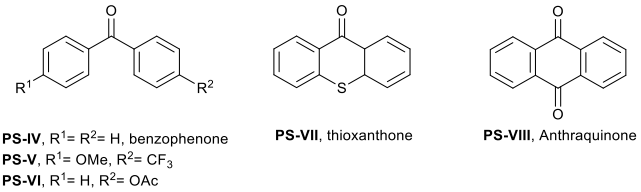

Figure 4. Examples of ketone-based photosensitizers used in metallaphotoredox catalysis.

3.3 Acridinium

Acridinium ions can be linked to a mesityl unit, as in **Mes-Acr$^+$** (**PS-IX**, Figure 5), to form a chromophore in which mesitylene is the electron donating group and acridinium the electron-accepting one. Upon photoexcitation with blue light, a charge transfer (CT) state (**Mes$^+$-Acr$^\bullet$**) can be efficiently populated. This state is then able to recombine to populate the triplet excited state T_1, localized on the acridinium moiety and displaying a lifetime of 5.3 ms at 77 K.[32] In recent years, the study and use of acridinium dyes has been extended significantly. Nicewicz has investigated the use of acridinium derivative **PS-X** (Figure 5) in photoredox catalysis.[33] If **PS-X**'s charge transfer state is quenched by a sacrificial electron donor, **Mes-Acr$^\bullet$** is formed and can be used as a potent reductant. The potential related to the oxidation of **Mes-Acr$^\bullet$** to **PS-X**, E(PS/PS$^{\bullet-}$), is –0.60 V vs. SCE in MeCN. On top of that, **Mes-Acr$^\bullet$** is colored with an absorption band between 450 and 550 nm in MeCN. Consequently, upon visible photoexcitation the reduced **Mes-Acr$^\bullet$** dye can reach an excited state whose oxidation potential, E(PS/*PS$^{\bullet-}$), is –2.91 V vs. SCE (in MeCN),[35] making **Mes-Acr$^\bullet$**'s reducing strength similar to that of alkali metals. However, the excited state of **Mes-Acr$^\bullet$** is a doublet (D_1) characterized by an extremely short lifetime (ca. 100 ps).[33] Consequently, its ability to promote photoredox reactions by bimolecular quenching mechanisms is highly disfavored: for example, in the case of diffusion-controlled processes with $k_q = 10^{10}$ M^{-1} s^{-1}, a quencher concentration of 0.1 M is required for a 10% quenching efficiency. Therefore, ground-state interactions between **Mes-Acr$^\bullet$** and the reaction partner are most likely responsible of the quenching process.

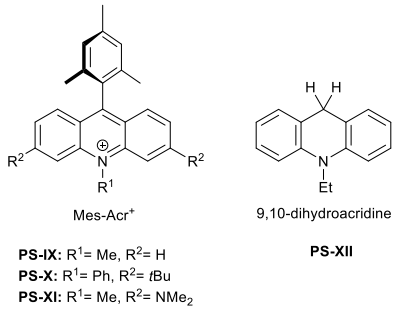

Figure 5. Acridinium-type photosensitizers.

3.4 Xanthene derivatives

Among xanthene derivatives, **Eosin Y** (**PS-XIII**, Figure 6) is the most commonly used in metallaphotoredox catalysis. This class of dyes is characterized by a strong absorption in the green region of the visible spectrum and, for example, **PS-XIII** has a molar absorption coefficient of 121000 $M^{-1}cm^{-1}$ at 542 nm.[34] Compared to the previously described classes of photosensitizers, it is therefore possible to use less energetic electromagnetic radiation for its excitation. Moreover, it is also possible to efficiently populate the triplet state of xanthene derivatives favoring the ISC process upon functionalization of their chromophore core with heavy halogen atoms (heavy atom effect). In the case of **PS-XIII**, the quantum yield for the population of the triplet state is 33% and its lifetime is 1.7 μs (in EtOH).[35] The reduction and oxidation potentials for this photosensitizer are modest compared with the previously described dyes and are, respectively, -1.14 and +0.72 V vs. SCE (in MeOH).[36] In **Rose Bengal** (**PS-XIV**, Figure 6), where the xanthene derivative bearing four iodine atoms around the core, ISC is even more favored and therefore the triplet state quantum yield is 61% (in EtOH).[35]

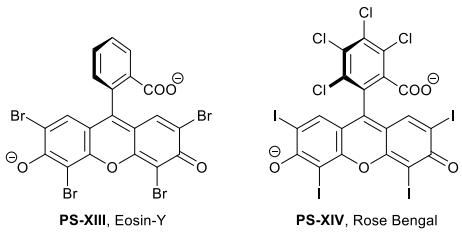

Figure 6: Xanthene-derived photosensitizers.

4. Organic dyes in photoredox nickel mediated processes

4.1. Carbazolyl-dicyanobenzenes dyes in nickel mediated processes

In 2016 a remarkable work reported carbazolyl cyanobenzenes (CDCBs) as a class of organic dyes in photoredox/Ni dual catalytic $C(sp^3)–C(sp^2)$ cross-coupling reactions. Zhang[37] and, successively Zeitler[27] have introduced a number of modification in the framework, by introducing halogens or changing the number and position of carbazolyl and cyano groups attached to the aromatic core. Cyanobenzene derivatives, and in particular **PS-I** (4CzIPN, Figure 3), have been extensively used in metallaphotoredox catalysis for two main reasons: a) the modification of the donor (carbazole or diphenylamine units) and acceptor (dicyanobenzene ring) groups can simply alter the oxidation and reduction potential, both in the ground and in the excited state; b) E_{00} can be simply modulated by these substituents; c) reversible voltammetric curves have been registered for these derivatives, highlighting the stability and reversibility of the different redox states of the PS.

For example, substituting one carbazole unit with a halogen substituent (**PSIII**, 3CzClIPN,Figure 3, it was possible to alter $E(PS^{\bullet+}/PS)$, which was increased from +1.49 V to +1.79 V (vs. SCE).[27] On the other hand, introducing EDG substituent on the carbazole ring (MeO groups) it was possible to modify the $E(PS^{\bullet+}/^*PS)$ from -1.18 V to -1.5 V vs. SCE.[27] In addition, the compounds are obtained by simple nucleophilic reactions (one step, in most cases), and further synthetic modifications are possible.[39] Not surprisingly these derivatives found a wide use in metal photoredox processes, in particular in nickel mediated reactions. Although the photoredox cycles in nickel mediated reaction is still under investigation[17] and different oxidation states of Ni are involved.[40] In order to form nickel catalyst in low oxidation state it is necessary a strong negative reduction potential of the photosensitizer in the fundamental state ($E(PS/PS^{\bullet-})$, where a reductive quenching is operative. In the case where an oxidative quenching is the photochemical event, an excited state oxidation potential of the photocatalyst $E(PS^{\bullet+}/^*PS)$ close to -1.2 v vs. SCE has to be provided. From many examples reported in the examined literature, it seems that the value of -1.2 v is generally obtained after a reductive quenching of the excited state of the organic photosensitizer, generating $PS^{\bullet-}$. Therefore, in many reported processes as discussed, the value of

E(*PS/PS•⁻) and E(PS/PS•⁻) needs to be tuned for a successful catalytic cycle. Zhang remarked that **PS-I** was both a strong oxidant and reductant in the excited state (E(*PS/PS•⁻)= +1.43 V vs. SCE; E(PS•⁺/*PS)= -1.18 V vs. SCE in MeCN), overcoming the possibilities offered by metal photosensitizer based on Ir(III) or Ru(II). The photoredox/Ni dual catalytic C(sp^3)−C(sp^2) cross-coupling[41] disclosed by Molander[15] and MacMillan/Doyle[14] was targeted (Scheme 1, A and B).[37]

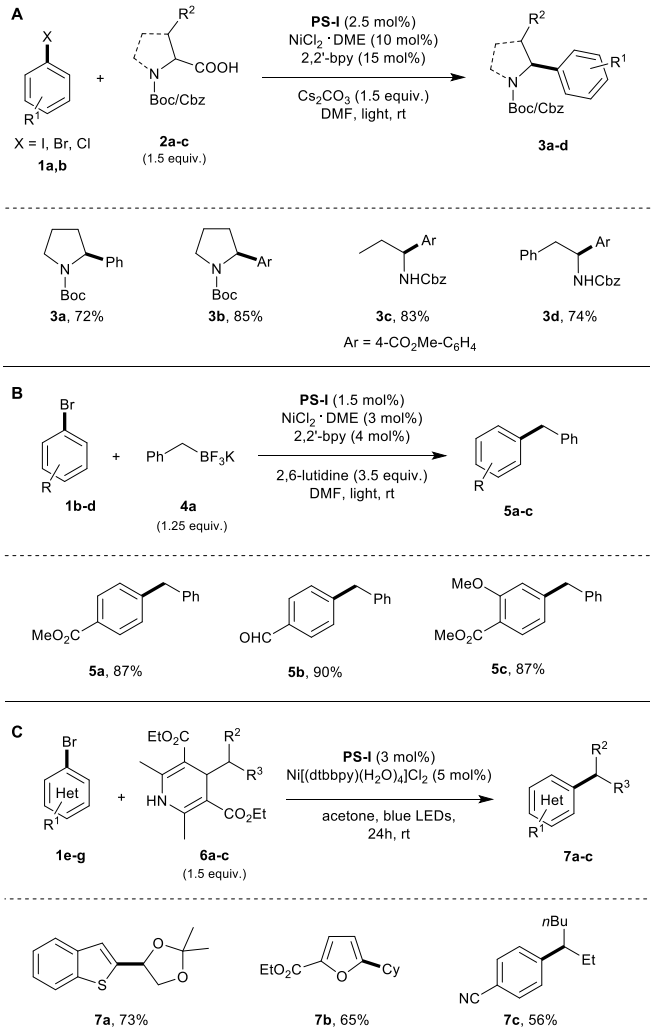

Scheme 1. Photoredox/Ni dual catalyzed cross coupling of aryl halides with carboxylic acid (A), trifluoroborates (B) and 1,4-dihydropyridines (C).

As in the case of the Ir(III)-mediated process, 4CzIPN presents a sufficient reduction potential in its excited state to generate the organic radical from the organic sp^3 precursor [E(*PS/PS•⁻)> +1.10 V vs. SCE]. After the electron transfer, the *PS is reductively quenched generating PS•⁻. The so-formed species is able to reduce the metal catalyst, forming a species of nickel in low oxidation state. Other organic dyes such as Eosin Y (**PS-XIII**), Rose Bengal (**PS-XIV**), methylene blue, and Mes-Acr⁺ (**PS-IX**) showed no activity, probably due to the lack of appropriate potentials. Molander reported in the same year[42] a Ni/photoredox dual catalytic cross-coupling employing (hetero)aryl bromides **1** with 1,4-dihydropyridines (DHP) **6** as source of C-centered radicals (Scheme 1, C), employing **PS-I** as active photoredox catalyst in this case as well. As often noted in sp^3 nickel coupling, the methodology is not suitable for primary alkyl or cyclopropyl derivatives, where the absence of the desired coupling product was observed. The process is promoted by a SET, via reductive quenching of the *PS. This yields the corresponding PS•⁻, a strong reductant that is able to reduce the nickel in right oxidation state. Alkylsilicates[43] were also employed in the presence of **PS-I** in cross coupling reactions promoted by nickel.[44] The mechanism is analogous to the one observed for 1,4-dihydropyridines and acid derivatives. The SET occurs between the excited state of the photosensitizer (*PS).

As an example of the fine tuning of the organic photosensitizer, Molander reported the synthesis of diverse flavanones **9** by coupling novel 2-trifluoroboratochromanone **8** with aryl and heteroaryl bromide **1**.[45] While Eosin Y (**PS-XIII**) and acridinium (**PS-IX**) were not able to promote the reaction, **PS-I** was found a productive sensitizer (Scheme 2).

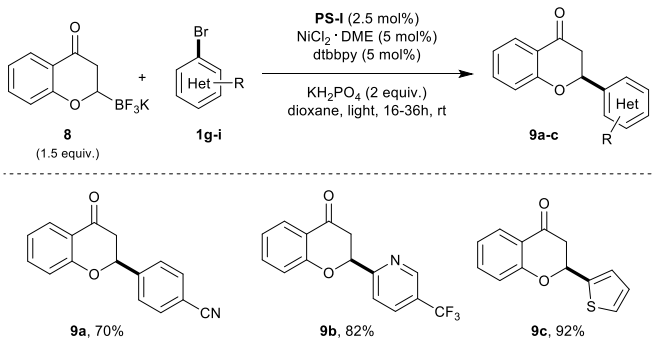

Scheme 2. Synthesis of flavanones via photoredox/Ni dual catalyzed α-arylation/heteroarylation of 2-trifluoroboratochromanones.[45]

Eosin Y (**PS-XIII**) has an insufficient potential (E(*PS/PS•−)) to promote the oxidation of trifluoroboratochromanone **8**, while the reduction potential (E(PS/PS•−)) of Mes-Acr+ **PS-IX** is not sufficiently low for the nickel reduction. Wang and Mariano described a formylation reaction of aryl halides, aryl triflates, and vinyl bromides under photoredox synergistic nickel catalysis, promoted by **PS-I**.[46] The formylation takes advantage of the simple oxidation of diethoxyacetic acid mediated by the excited state of **PS-I**. The process can be directly applied to the synthesis of aromatic aldehydes bearing different functional groups. The incorporation of C-glycosides in drug design was considered by Molander,47 who described the preparation of C-acyl glycosides **12** through a Ni/photoredox dual catalytic processes, again using **PS-I** as photosensitizer (Scheme 3, A).

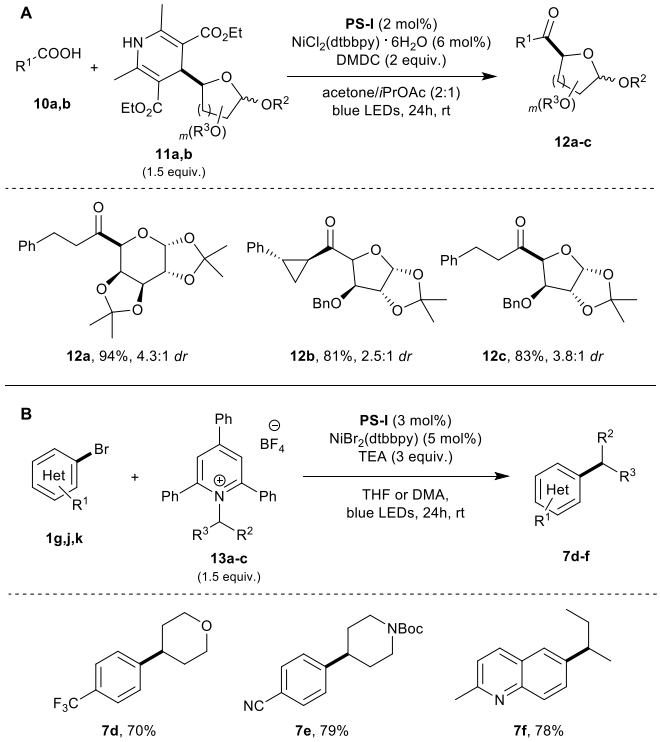

Scheme 3. Ni/photoredox dual catalyzed (A) acylation of C-glycosides and (B) arylation/heteroarylation of electrophilic Katritzky salts.[47]

1,4-Dihydropyridines **11** were employed as glycosyl radical precursor, generated by reductive quenching of the excited state of the PS. In order to have direct access to acyl derivatives, in situ activated carboxylic acids **10** by dimethyl dicarbonate (DMDC) were selected as reaction partners. DMDC was chosen to be employed after an intense experimentation and evaluation of activating different agents. Although a mechanistic picture was not provided, the reaction is probably occurring via formation of an acylnickel intermediate that is intercepted by the glycosyl radical to form the corresponding Ni(III) intermediate, leading to the observed product after reductive elimination.

DNA-encoded library (DEL) technology is widely used in pharmaceutical industries[48] and in order to expand the diversity within the sp^3 functionalization, photoredox catalysis can be the right tool. In fact, Molander[49] has reported the possibility of merging Ni/photoredox dual catalysis in useful $C(sp^2)$–$C(sp^3)$ cross-coupling as well as photoredox-catalyzed radical/polar crossover

alkylation protocols with DELs. One of the major problems associated with these compounds is the poor solubility of the modified DNA molecules. The use of high dilution and excess of the reagents (40−1000 equiv.) solved this problem. Pre-catalysts and additives were important reaction parameters to consider in this chemistry. 4CzIPN (**PS-I**) was found to be the most suitable photosensitizer, considering the redox potential (E(DHP$^{\bullet+}$/DHP) = +1.10 vs. SCE) necessary to generate an alkyl radical from alkyl 1,4-dihydropyridines (DHPs) and acids derivatives, employed as alkyl radical source. Various aryl or heteroaryl halides were bonded via amide bonds to DNA, to accomplish the desired couplings. Katritzky salts **13**, formed via a simple condensation of the corresponding primary amines with a bench-stable, commercially available triphenylpyrylium was used as suitable precursor alkyl radicals, in various cross coupling reactions.[50] Katritzky salts, indeed, form alkyl radicals via a single electron reduction process[58a] and subsequent fragmentation. Molander reported a cross-electrophilic coupling via Katritzky salts **13**[47b] (Scheme 3, B) with a Ni/photoredox dual catalysis. 4CzIPN (**PS-I**) was employed as photosensitizer in this dual process, in this case. However, the mechanism was found to be slightly different compared with the previously mentioned ones. Stern-Volmer experiments confirmed that the excited state of the photosensitizer is reductively quenched by triethylamine, the sacrificial reagent. The excited state of the PS has a sufficiently negative reduction potential (E(*PS/PS$^{\bullet-}$)= +1.35 V vs. SCE) to oxidize triethylamine (E(A$^{\bullet+}$/A)= +1.0 V vs. SCE).[51] The quenching event generates PS$^{\bullet-}$ with a more negative reduction potential (-1.21 V vs. SCE) with respect to the Katritzky salt (E(A/A$^{\bullet-}$)= −0.93 V vs. SCE).[47b] The authors do not exclude in the paper that the reduction could be promoted by nickel in low oxidation state generated during the reaction. The classical Ni(I)/Ni(III) pathway was proposed for the cross coupling, with the reduced state of the catalyst (PS$^{\bullet-}$) able to reduce nickel to the low oxidation state.
Oxa and azabenzonorbornadienes **14** (Scheme 4) were examined by Guitierrez and Molander as possible electrophilic partners in a photoredox/nickel reaction in order to have access to interesting 2-alkyl-1,2-dihydronaphthalenols **15**.[52]

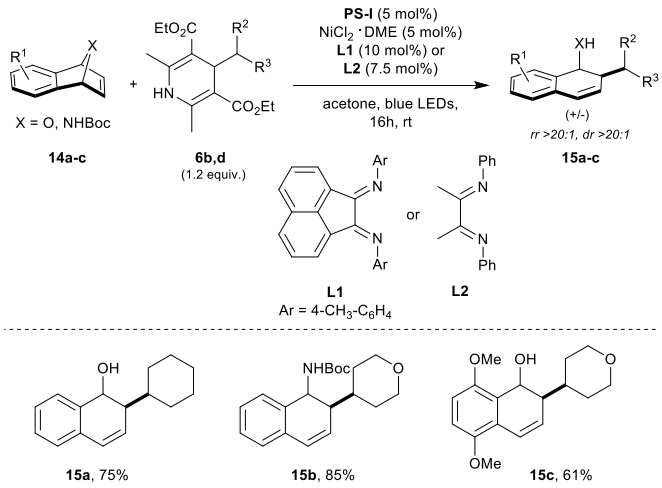

Scheme 4. Ni/photoredox dual catalyzed alkylation of Oxa and azabenzonorbornadienes.[52]

Due to the difficulties related to the study of the mechanism of metallaphotoredox catalytic reactions, density functional theory (DFT) calculations were employed to gain some insight about the possible mechanistic picture. Basically, the excited state of **PS-I** is reductively quenched by 4-alkyl-DHP **6** to form **PS**$^{\bullet-}$, which is able to generate Ni(0). Interaction of Ni(0) with epoxy or aziridine moieties gives Ni(II) allyl complexes. Radical generated by fragmentation of the reduced 4-alkyl-DHP **6** interacting with Ni(II) gives the corresponding Ni(III) adduct. As reported in other calculations[53] the reaction is barrierless and reversible. This peculiar behavior is important in other mechanisms, as the radical produced in the reversible step can participate in hydrogen atom transfer (HAT) processes. Thanks to an effective reductive elimination, the desired products are formed.
The interesting photoredox Ni-catalyzed cross-coupling between tosyl-protected alkyl aziridines **16** and commercially available (hetero)aryl iodides **1**, to access phenethylamine derivatives **17**, was described by Doyle[54] with the employment of **PS-I** as photosensitizer (Scheme 5).

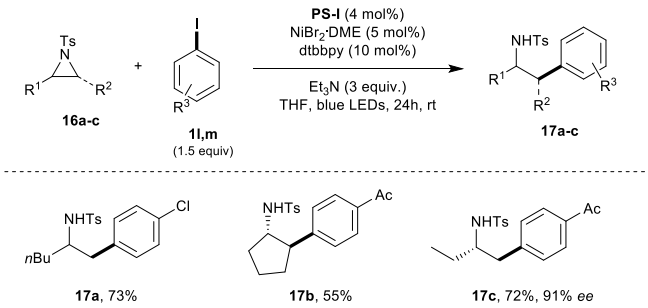

Scheme 5. Photocatalytic Ni-catalyzed ring opening of tosylaziridines with (hetero)aryl iodides [54]

Mechanistically, the reaction is determined by the formation of reduced Ni(0), capable of giving oxidative addition with the aryl iodides. In situ generated hydriodic acid promotes the aziridine opening to the corresponding iodoamine. The iodo derivatives through a SET event followed by fragmentation, mediated by various possible precursors ([dtbbpy]Ni(I) complex or PS^-), intercepted by Ni(II) complex. In the above-mentioned example reported by Doyle the possibility – arising from the reversible radical generation – of performing a HAT catalytic cycle was disclosed. This has been clearly shown by Paixão and König, that recently reported a C(sp^3)-C(sp^3) cross-coupling of alkyl bromides and alkyl chlorides **18** with ethers **19** by dual photoredox/nickel catalysis promoted by **PS-I** (Scheme 6).[55]

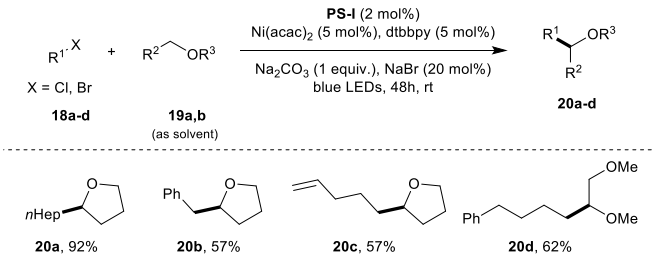

Scheme 6. C(sp^3)-C(sp^3) cross-coupling of alkyl bromides and chlorides with ethers by dual photoredox/Ni catalysis promoted by 4CzIPN.[55]

The mechanistic proposal followed the previous discussions, with alkyl bromide undergoing an oxidative addition on the Ni(0) complex to give a Ni(II)-alkyl halide complex. As pointed out in the several examples here illustrated, the reduction of Ni(II) to Ni(0) is supposed to occur via SET from the reduced photosensitizer ($PS^{\bullet-}$). The now-formed LNi(II)BrR is oxidized to LNi(III)BrR by the photosensitizer **PS-I** in its excited state [E(*PS/$PS^{\bullet-}$)= +1.35 V vs. SCE in CH_3CN]. As discussed previously, Ni(III) can give LNi(II)R and Br radical in a facile manner. At this point the electrophilic bromine radical can behave as HAT agent and is capable of abstracting hydrogen atom from species with low BDE in the reaction mixture. Due to the presence of ethers, the abstraction of the hydrogen atom from the carbon adjacent oxygen is favored. The formation of a carbon-centered radical in α position to oxygen is followed to the addition to Ni(II) generating Ni(III) intermediate, that gave the observed compounds after reductive elimination.
The conditions required for the Ni(II)/photoredox catalyzed coupling in the presence of organic dyes can allow the possible preparation of useful chiral intermediates, such as enantioenriched allyl carbamates **22**.[56] Starting from chiral 1-bromo-alken-3-ol derivatives **21**, it is possible to alkylate alkylbromides **18** bearing different functional groups (e.g. CN, Ar, epoxide, Cl, Bpin, OTHP, SO_2Ph, alkyne, COOR, Ph) in high chemoselective manner (Scheme 7).

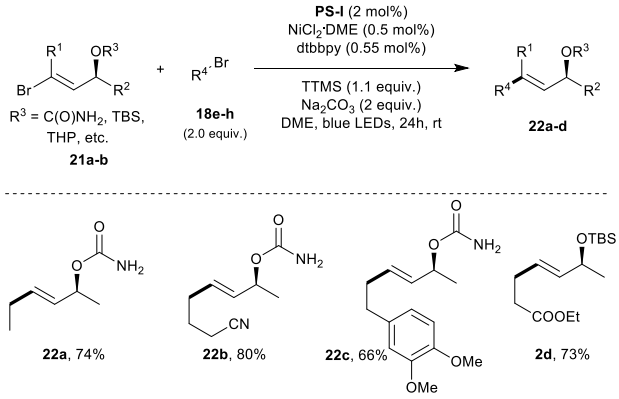

Scheme 7. Photoredox/Ni-catalyzed cross-coupling alkylation of chiral 1-bromo-alken-3-ol derivatives.[56]

The utility of the protocol was demonstrated with the preparation of allylamine derivatives through sigmatropic rearrangement. The synthesis of amides is an important topic in organic synthesis and efforts to develop functional schemes for their preparation through synergistic dual photoredox catalysis were reported. This is related to the common methodology used to access amides, which normally consists in the use of coupling reagents or in metal-mediated reactions with insertion of toxic CO.[57] An interesting methodology that uses nickel in combination with **PS-I** for preparing amides was recently disclosed by Melchiorre (Scheme 8).[58]

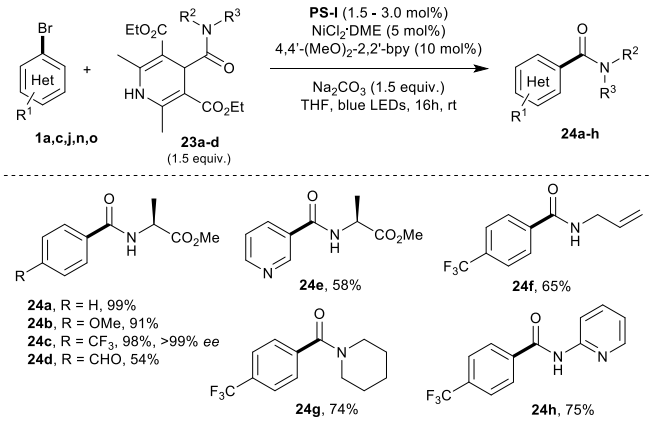

Scheme 8. Photoredox/Ni-catalyzed carbamoylation of (hetero)aryl bromides for amides synthesis.[58]

The radical source used in this process was the readily available, cheap and stable 4-carbamoyl-1,4-dihydropyridines **23** which, via SET oxidation with the **PS-I** photosensitizer, can generate the corresponding carbamoyl radicals. These are intercepted by nickel with the usual scheme. A possible mechanism was suggested for the Ni/photoredox-catalysed carbamoylation reaction. The excited state photosensitizer is a strong enough oxidant to extract an electron from dihydropyridine ($E(DHP^{\bullet+}/DHP)$= +1.39 V vs. Ag/Ag^+ in CH_3CN) which, after fragmentation, gives the carbamoyl radical. The so-formed radical then reacts with the Ni(II)ArBr intermediate to form Ni(III) species, and the reductive elimination gives the final product.
The photoredox Ni-mediated processes in the presence of **PS-I** can be extended also to multicomponent reactions as exemplified by two quite recent examples. In the first cascade reaction, reported by Noble and Aggarwal[59] (Scheme 9), the synthesis of functionalized alkyl boronic esters **26** was realized. Cross-coupling of vinyl boronic ester **25** with carboxylic acids **2** and aryl iodides **1**, in the presence of Ni(II) catalyst, was reported with an excellent functional group tolerance.

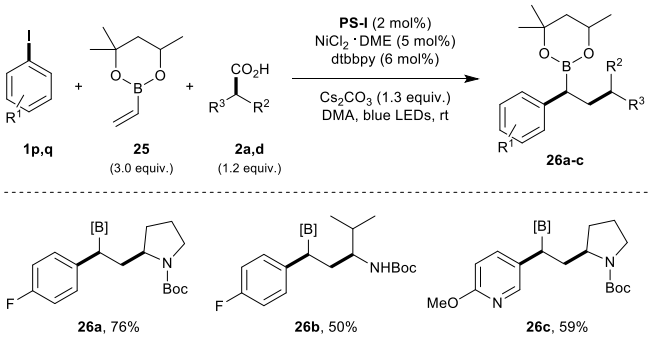

Scheme 9. Synthesis of functionalized alkyl boronic esters via metallaphotoredox catalyzed conjunctive cross-coupling.[59]

Various carboxylic acids were employed and an application to the synthesis of sedum alkaloid was also described. The main limitation of this method is related to the employment of electron deficient aryl iodides, that gave boronic esters which are unstable under the reaction conditions. The authors proposed that the intermediate α-boryl radical, generated by the addition of alkyl radical to vinyl boronic ester, is intercepted by the Ni(II)ArBr complex, affording the observed product after reductive elimination. In order to favor the desired crossed product, a careful selection of the starting carboxylic acid **2** was made.[59]

4.1.1 Enantioselective photoredox processes with organic dyes and nickel catalysis.

Although the combination of photoredox catalysis with enantioselective transformation is quite challenging, pioneering examples have been recently reported, and will certainly attract more work in the future.[60] Chiral Ni(III) intermediate surrounded by appropriate ligand can give, due to the reversibility of the radical addition, several advantages compared with other metals to construct stereoselective transformations.[61]

A few interesting examples of stereoselective processes in which **PS-I** was employed as active organic dye in a stereoselective process were recently reported. Doyle and Rovis groups presented the asymmetric Ni-catalyzed desymmetrization of *meso*-succinic anhydrides **27** using benzyltrifluoroborates **4** as the alkyl radical source, in the presence of **PS-I** as organic photosensitizer (Scheme 10, A).[62]

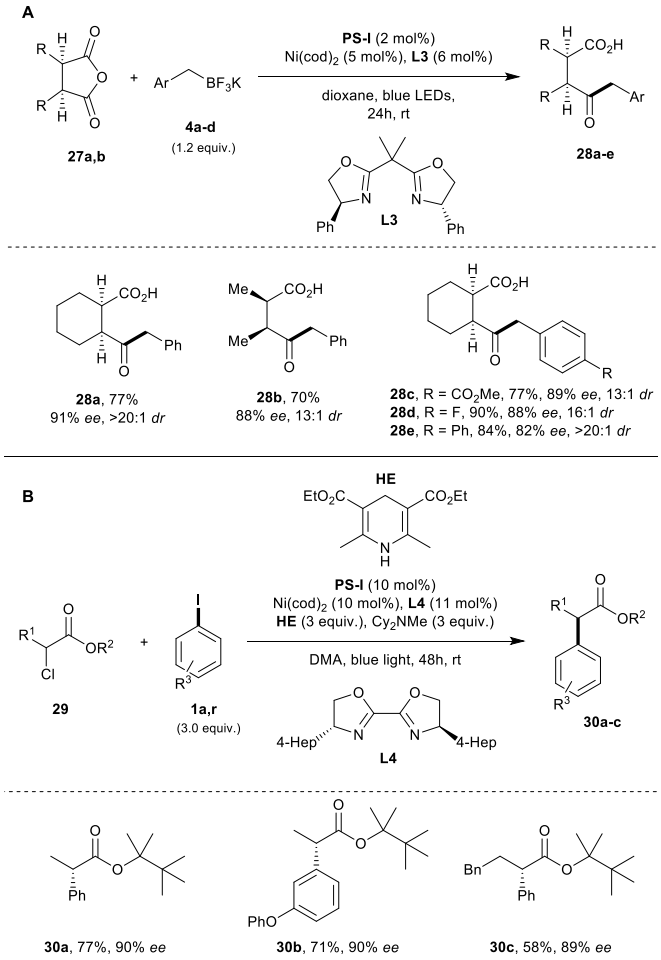

Scheme 10. (A) Ni/photoredox-catalyzed desymmetrization of *meso*-succinic anhydrides; (B) Ni/photoredox-catalyzed asymmetric reductive cross-coupling of α-chloro esters with aryl iodides.[62]

Photophysical studies provided the evidence that an oxidative addition process occurred before the radical addition to a Ni(II) intermediate. The above-mentioned results can be justified due to the fact that the process is energetically favored. One drawback is related to the use of sensitive $Ni(COD)_2$ as pre-catalysts.

Walsh and Mao[63] employed **PS-I** as photosensitizer, in the presence of Hantzsch ester (**HE**) as the terminal organic reductant for a catalyzed asymmetric reductive cross-coupling of α-chloro esters **29** with aryl iodides **1** for the simple and effective preparation of α-aryl esters **30** (Scheme 10, B). The chiral ligand used for the transformation is a quite simple and readily available modified bis-oxazoline (BiOX) (**L4**, Scheme 10). According to the mechanistic proposal LNi(II) complex, formed in situ, is reduced to LNi(0) by the $PS^{\bullet-}$ which is previously obtained by reductive quenching of the **PS-I** by the sacrificial Hantzsch's ester (**HE**). The reduction of the chloroester and the concomitant formation of the corresponding stabilized α-radical species can be carried out by different reductants (the oxidized HE, the LNi(I) complex or the $PS^{\bullet-}$) and the authors cannot make a distinction or have evidence for conclude which process is favoured.

Xiao designed a chiral BOX ligand linked to a thioxanthone moiety (**L5**, Scheme 11, A) to carry out an aerobic oxidation of keto esters and ketoamides **31**.[60b]

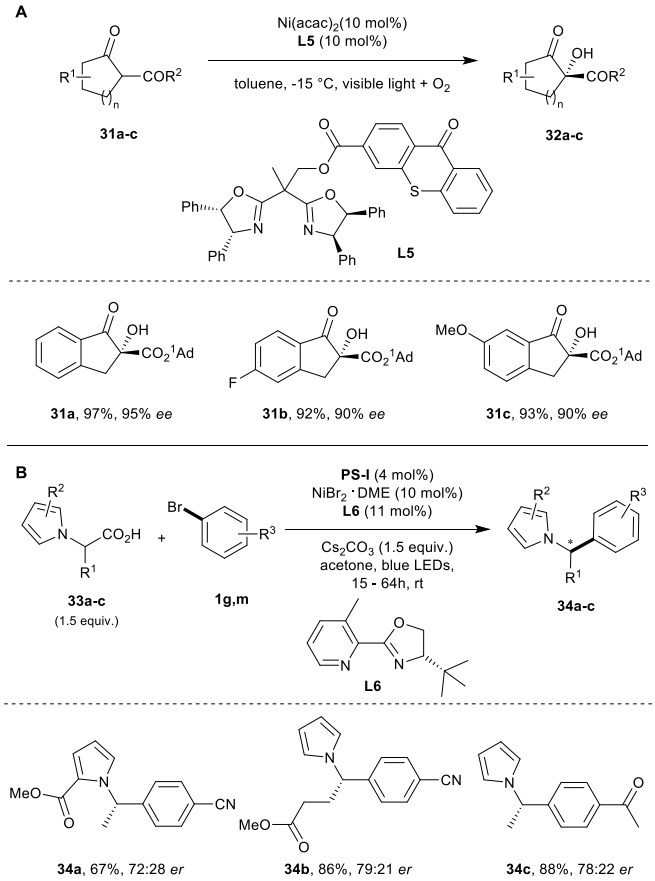

Scheme 11. (A) Enantioselective aerobic asymmetric oxidation of β-ketoesters via chiral Ni-catalyst complex; (B) enantioselective Ni/photoredox cross-coupling arylation of α-heterocyclic carboxylic acids.[64]

The proposed mechanism for this stereoselective transformation, is different from the ones reported so far. Here, the thioxanthone is acting as triplet state photosensitizer of oxygen, forming singlet oxygen. This species is capable of oxidizing the ketoester into the corresponding hydroxy dicarbonyl compounds. Finally, Davidson and Bonifazi have described an enantioselective synthesis of *N*-benzylic heterocycles from stabilized carboxylic acids using an organic photosensitizer and a chiral pyridine-oxazoline ligand (**L6**, Scheme 11, B) again employing **PS-I**.[64.] α-heterocyclic carboxylic acids **33** were used as precursor of radicals in a decarboxylative strategy.

4.1.2 Activation of CO_2 with organic dyes and metallaphotoredox catalysis.

To conclude this section about the use of **PS-I** a particular mention goes to the application of organic photosensitizers in activation of CO_2 with dual catalysis. The ability to reduce CO_2 and transform this inactive molecule in a reagent is coupled with nickel for the incorporation of activated CO_2 in organic molecules. In this perspective, König reported an effective carbonylation of aryl and alkyl bromides and triflates **35** with CO_2 in combination with a nickel complex (Scheme 12).[65]

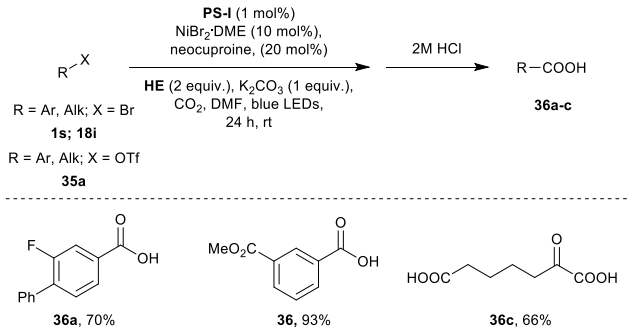

Scheme 12. Ni-photocatalyzed carboxylation of bromides and triflates with CO_2.[65]

Interesting spectroscopic and mechanistic studies were able to shed light on the process, by the use of spectroelectrochemistry. The reduction by $PS^{\bullet-}$ of the Ni(II)-neocuproine complex take place step-wise to give two species [NI(I) and Ni(0)]. The neocuproine-Ni(0) interacts with the bromides via oxidative addition and forms the LNiBrR species. These can be further reduced to the corresponding LNi(I)R intermediates. At this stage, the interaction with CO_2 takes place, forming the LNi(III)R(CO_2) complex that, after reductive elimination, gives the observed carboxylate. König, in a successive study[66] described the carbonylation of styrene derivatives, and how the reaction can be controlled by ligands on the nickel complex. The ligand-controlled Markovnikov and anti-Markovnikov hydrocarboxylation of styrenes was performed in the presence on Ni(II) and **PS-I**, under visible light irradiation. The Markovnikov product (α-benzyl carboxylates) was obtained with cuproine, while with 1,4-bis-(diphenylphosphino)butane (dppb) as ligand the anti-Markovnikov product was isolated. A variety of differently substituted styrene derivative by electron rich or poor substituents can be employed in the process. Mechanistically, the reaction is intriguing. The employment of **HE** ester is crucial because, by decomposition, a proton is formed. This proton can react with the Ni(0) complex, affording the corresponding nickel hydride. Hydrometallation of the styrene by the HNi(I)L is responsible for the formation of the nickel complexes involved in the transformation, in the case of Markovnikov product. The anti Markovnikov product is due to the ability of the phosphine ligand to allow the direct coordination of CO_2 to the Ni(0) complex, followed by insertion of styrene. In both cases, the Ni(II) complexes obtained are reduced to Ni(I) complex by the $PS^{\bullet-}$.

4.2 Ketones PS in nickel dual catalysis.

As specified in our simplified introduction aryl ketones can be excited via an $n \rightarrow \pi^*$ excitation process, that rapidly interconverts the sensitizer into a triplet state. This state is able to mediate eT reactions and, at the same time can mediate HAT reactions.[67] Murakami reported the direct homocoupling of arylbromides promoted by catalytic amount of thioxanthone in the presence of Ni(II), dtbbpy (4,4'-di-*tert*-butyl-2,2'-bipyridine) as a ligand and using Et(*i*Pr)$_2$N as sacrificial reductant.[68] The thioxanthone receives an electron in its excited state from Et(*i*Pr)$_2$N, forming the reduced ketyl radical anion. The radical anion is able to reduce Ni(II) to Ni(0) complex. The Ni(0) complex is able to engage in an oxidative addition with aryl bromide giving LArNi(II)Br. Disproportion of Ni(II) complex was evoked to explain the formation of Ni(II)Ar$_2$, followed by reductive elimination. An interesting employment of the triplet ketone sensitizers, that combines hydrogen-atom transfer (HAT) and single-electron transfer (SET) processes, was reported by Martin (Scheme 13, A).[30]

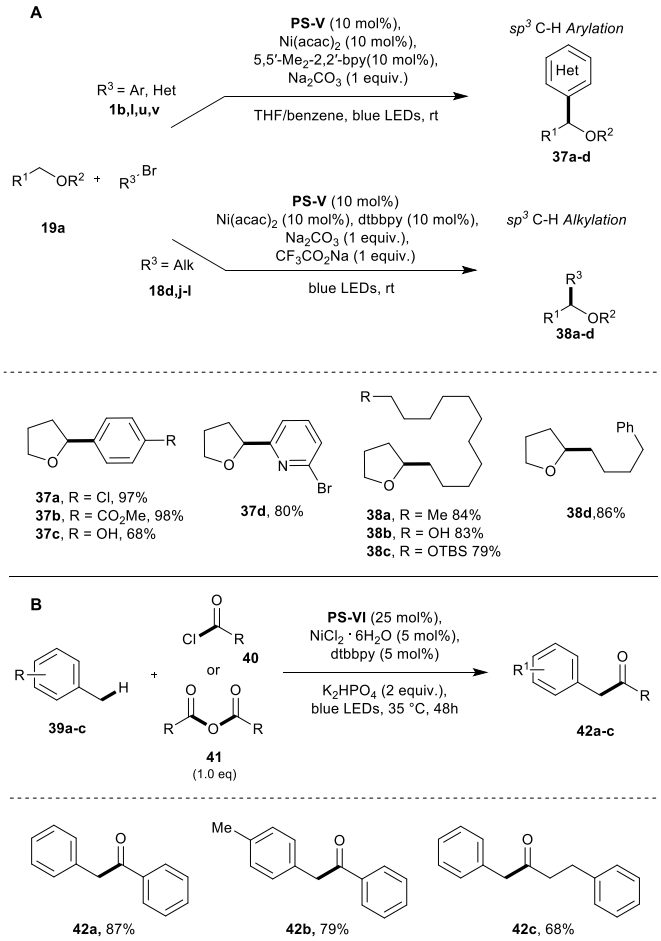

Scheme 13. Combination of triplet excited ketones and nickel complex in a dual catalytic reaction for (A) C(sp^3)−H arylation and alkylation and (B) synthesis of unsymmetrical ketones through acylation of C(sp^3)−H benzylic bonds.[30,70]

The methodology was applied to the direct C(sp^3)–C(sp^2) and C(sp^3)–C(sp^3) bond construction using abundant alkanes as starting material, in the presence of Ni(II) salt and ketones as photosensitizer. The structure of the ketone photosensitizer was optimized, and the compound **PS-V** was found to be the most effective PS for the reaction. Inexpensive and simple 5,5'-dimethyl-2,2'-bipyridine was the ligand employed in the study. The reaction used mainly different cyclic and acyclic ethers **19** as starting materials, due to the low dissociation energies (BDEs) of the C-H bond close to the oxygen atom, although examples of employment of cyclohexane was also included. Mechanistic studies were quite informative. Deuteration studies excluded the formation of bromine radical from Ni(II) complexes. The isolated ArNi(II)Br complexes were found to give the desired product if irradiated and only in the presence of the ketone PS. Finally, electronic spin resonance (EPR) spectra shown the presence in the reaction mixture of Ni(I) complexes and ketyl radical. All data together are pointing to a mechanism in which the triplet state of the photosensitizer generates a radical from the substrate by HAT and the so-formed ketyl radical is able to reduce the Ni(II)(acac)$_2$ complex used in the transformation to a Ni(0) form. Then the reaction proceeds via oxidative addition of the LNi(0) complex to bromide derivative to form the corresponding LRNi(II)Br complex, which is able to intercept the radical organic species formed by HAT. The final step is the reductive elimination, with re-generation of Ni(I) that closes the catalytic cycle. By taking advantage of the mentioned HAT ability of ketyl radical anion, two synthesis of ketones were described. König reported a dual catalytic arylation of aromatic aldehydes with aryl bromides using UV-irradiation and a nickel catalyst.[69] Formation of the acyl radical is determined by a HAT reaction between the ketyl radical anion of the photosensitizer and the aromatic aldehydes. Dewanji and Rueping reported[70] the preparation of unsymmetrical ketones **42** by a nickel dual catalytic system (Scheme 13, B). The direct benzylic C–H acylation of toluene, methylbenzene or other similar derivatives **39** was possible in the presence of different acid chlorides **40** and anhydrides **41**. The mechanism is quite close to the previously discussed. The only difference encountered is related to the in situ formed LNi(0) (L = dtbbpy). In this case the species can perform the oxidative addition with the acylderivative to give the LNi(II)acyl complex, which is able to react with the benzyl radical obtained in the HAT step with the ketone photosensitizer in its excited state.

4.3 Acridinium dyes employed with nickel metallaphotoredox catalysis.

Acridinium catalyst **PS-IX** (Figure 5) is a strong oxidant, and a moderate reductant. Its accommodation in dual catalysis with nickel was realized through interesting new concepts. Kanai recently reported an acceptorless dehydrogenation of aliphatic secondary alcohols **58** to ketones **59a-d** under visible light irradiation, in the presence of a ternary catalytic system, that uses nickel catalysis, HAT mediator and BINOL thiophosphate (**CAT1**, Scheme 14, A).[71] The reaction is thought to proceed through the formation of the thiyl radical by oxidation of **CAT1** by the acridinium photosensitizer, and subsequently by HAT from the α-C–H bond of the alcohol substrate to form a radical species. This radical is intercepted by the NI(II) complex, to form the corresponding Ni(III) derivatives. After reduction of the Ni(III) intermediate to Ni(II), operated by the PS•⁻ photosensitizer, and a β-hydride elimination, enol form of the ketone is obtained, that tautomerizes into the desired product.

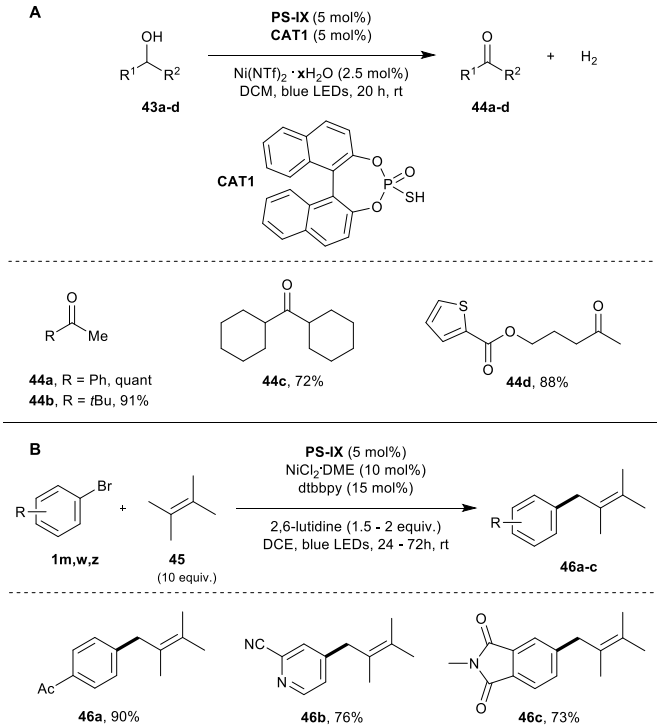

Scheme 14. (A) Ternary hybrid catalysis comprising a photoredox catalyst, an organocatalyst, and a nickel catalyst for dehydrogenation of aliphatic alcohols to ketones; (B) dual Ni/photoredox catalyzed cross-coupling of allylic C(sp³)-H bonds with aryl and vinylbromides.[71,72]

Another concept used with acridinium photosensitizer **PS-IX** and nickel was reported by Rueping. The author described a direct allylation of aryl bromides by a dual nickel mediated photocatalytic process (Scheme 14, B).[72] The formation of Ni in low oxidation state is unlikely in this process, as PS•⁻ formed by a supposed oxidation of alkenes by the *PS, has a value that is thermodynamically unfavorable for the nickel reduction (E(PS/PS•⁻)= –0.57 V vs. SCE). Generation of species able to perform an HAT process, was responsible for the formation of the allyl radical. The bromine radical was formed upon energy transfer from the *PS to the ArNi(II)Br species. The obtained *[ArNi(II)Br] species is fragmented in Br radical and Ni(I). Br radical by HAT is responsible for the formation of the allyl radical, intercepted by ArNi(I) species to form the Ni(II)allylaryl derivative, that, after reductive elimination, gave the observed product **46**.

Another interesting concept introduced by Rueping with acridinium **PS-IX** in the presence of nickel, regards the use of cyclic alcohols **47** for the remote and site-specific arylation of ketones via the combination of photoredox and proton coupled electron transfer (PCeT) (Scheme 15).[73] The mechanism of the reaction was presumed to be radical thanks to experiments carried out with radical clocks and TEMPO. Then, the formation of hydrogen bond between the base and alcohols was shown by NMR spectroscopy. The oxidation of the electron rich arene moiety caused by acridinium in its excited state is followed by proton-coupled electron transfer (PCET) form an oxygen centered radical species. This undergoes the generation of the associated ketones, via C–C bond cleavage with the formation of a carbon centered radical. This radical is intercepted by the nickel-based cycle, as was illustrated in the discussed examples.

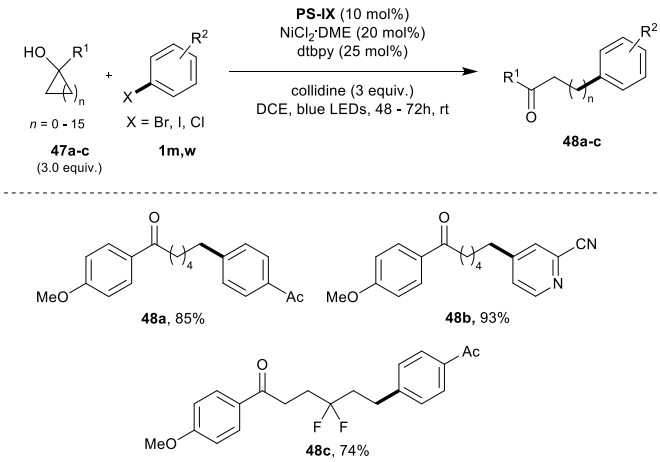

Scheme 15. Remote and site-specific arylation of ketones from cyclic alcohol through the combination of Ni/photoredox catalysis and proton-electron transfer.[73]

4.4 Other dyes as photosensitizers in dual nickel metallaphotoredox catalysis.

Just to underline the difficulties related to the development of metallaphotoredox catalytic processes, only a couple of examples were reported with organic dyes different from 4CzIPN and acridinium (**PS-I** and **PS-IX**). Modified heteroanthrylium dyes were described by Sparr[74] with a modular method starting from available precursor (Scheme 16, A).

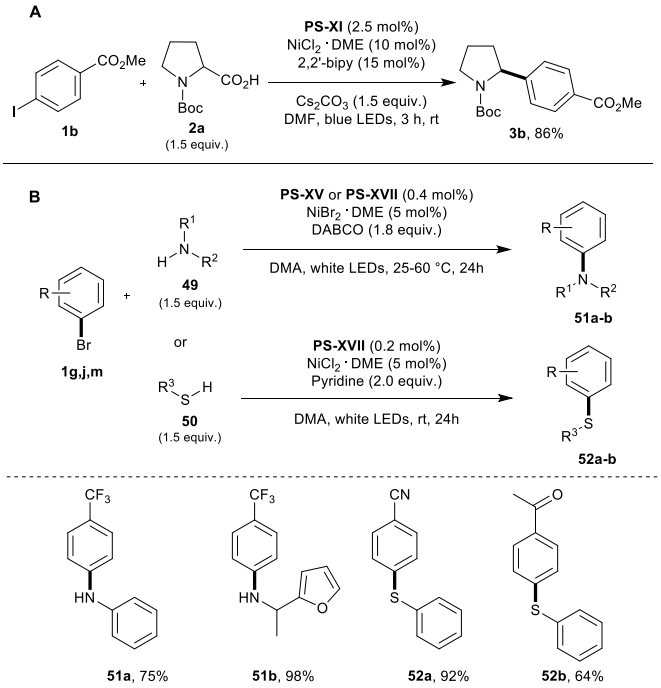

Scheme 16. (A) Dual photoredox/Ni catalysis cross-coupling of Boc-proline with methyl 4-iodobenzoate; (B) Dual photoredox/Ni catalyzed C–N and C–S cross-coupling reaction with aryl bromides using phenazine photosensitizers.[74,75]

A modified diaminoacridinium dye **PS-XI** (Figure 5) was able to promote a standard coupling between *N*-Boc proline and methyl 4-iodobenzoate in a nickel mediated process. Diaminoacridinium dye **PS-XI** gave the desired product in high conversion, while Mes-Acr$^+$ **PS-IX** or Eosin **PS-XIII** were completely inefficient. Miyake reported (Scheme 16, B) the use of *N*,*N*-5,10-di(2-naphthalene)-5,10-dihydrophenazine (**PS-XV**, Figure 7) and 3,7-(4-biphenyl)-1-naphthalene-10-phenoxazine dyes (**PS-XVII**, Figure 7) for the construction of C–N and C–S in combination with nickel catalysis.[75]

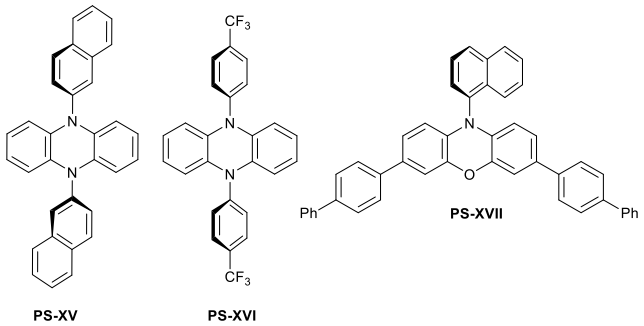

Figure 7. Phenazine derivatives photosensitizers.

5. Organic dyes in photoredox cobalt-mediated processes.

5.1 Reactions promoted by Eosin.

A great challenge, for photoredox/transition metal dual-catalysis, is about the use of cheap, abundant, low toxic metals to promote innovative transformations. The dual catalytic approach that considers cobalt in interesting transformations is still underdeveloped,[76] although many studies have been applying transition metal based photoredox catalysis for such transformations. Nevertheless, some interesting reports were published in recent years.

Sundararaju and co-workers reported a cobalt dual photoredox C−H activation protocol involving the use of Eosin Y (**PS-XII**, Figure 6) as photosensitizer (Scheme 17).[77] By tailoring the aromatic substrate **53** with a directing group, the procedure allowed the C−H and N−H bond annulation, with the presence of oxygen as the terminal oxidant. The photocatalysis is based on the well-established concept of C−H functionalization with high valent electrophilic cobalt complexes. Isoquinolones **55** are obtained in good yields and regioselectivity, with various unsymmetrical alkynes **54**. Mechanistically, the reaction was proven to occur via an electron transfer. By ligand exchange, a Co(II) coordinated to the directing group was formed. This complex was oxidized by the excited state of Eosin. The formation of the electrophilic Co(III) gave the cyclometallation of the aromatic substrate. This step is rate-limited, as proven by isotopic effect. The cobalt-coordinated alkyne gave the regioselective insertion, followed by reductive elimination. The catalytic cycle of the photosensitizer is closed by oxygen, that oxidizes $PS^{\bullet-}$.

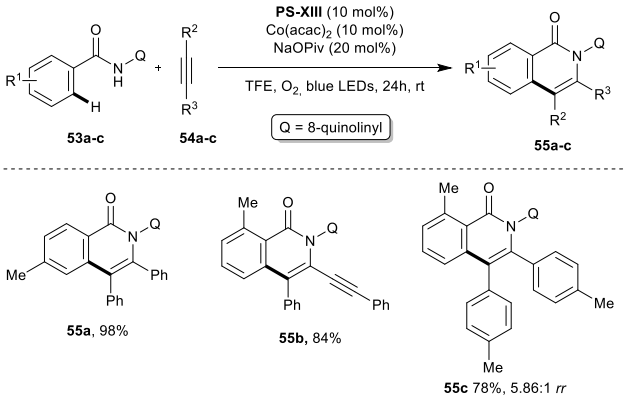

Scheme 17. Co/photoredox catalyzed C−H and N−H annulations of benzamides.[77]

Rueping and Sundararaju have reported[78] a quite similar reaction where aryl amides, bearing the same directing group, were used in a dual catalytic approach for the C–H and N–H bond annulation with alkenes under mild conditions. High regioselectivity was manifested using various terminal olefins with excellent functional group tolerance. Moreover, in this reaction, the involvement of superoxide radical anions and single electron transfer from Eosin's excited state were confirmed, with the mechanism of the reaction closely resembling the aforementioned one. Different substrates were used for a reaction that showed a good scope and the possibility of applying the protocol directly to compounds isolated from natural sources.

5.2 Reactions promoted by 4CzIPN.

A thermodynamic and kinetic isomerization of alkenes **56-58** can be obtained by the combination of **PS-I** and $Co(acac)_2$, by irradiation with visible light (Scheme 18, A).[79]

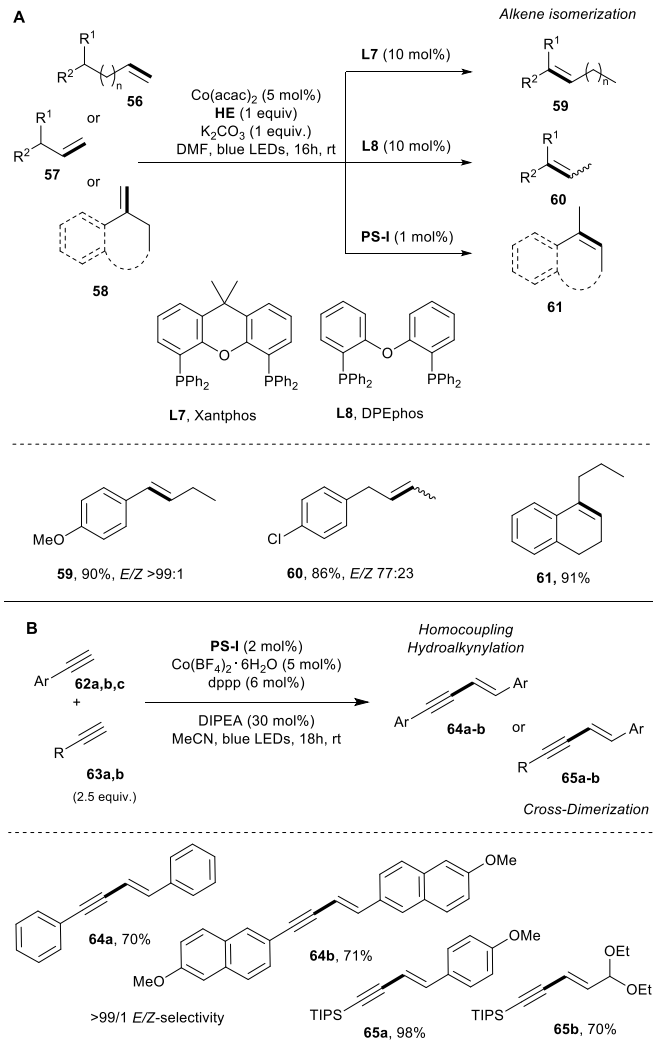

Scheme 18. Application of Co/photoredox catalysis in the (A) isomerization of alkenes and (B) hydroalkynylation for the synthesis of 1,3-enynes.[79,81]

The obtainment of the more or less substituted alkenes is a function of the ligand employed. Utilizing Xantphos (**L7**, Scheme 18, A) as the ligand, the most stable isomers were obtained, while isomerizing terminal alkenes over one position were selectively formed by using DPEphos (**L8**, Scheme 18, A) as the ligand. The scope of the reaction was excellent, and the yields were in general quite high, employing both the described conditions. The mechanistic picture proposed for the reaction considers the excited state of **PS-I** (Figure 3) reductively quenched by HE. The so-formed $PS^{\bullet-}$ state can reduce Co(II) to Co(I). On the other hand, HE is also a strong reductant in its excited state [E(*HE/$HE^{\bullet+}$) = −2.28 V vs. SCE].[80] and it is not excluded that excited HE ester can donate electrons to cobalt. Co(I) is surrounded by phosphines present in the reaction mixture and it is transformed in LCo(III)H hydride complex by reaction with H^+ (H^+ is derived by decomposition of HE ester after the first reductive events). Reaction of the LCo(III)H complex with alkene forms the corresponding LCo(III)alkyl complex. The isomerization occurs by β-hydride elimination, probably facilitated by irradiation of the reaction mixture.

An interesting photochemical hydroalkynylation for the synthesis of 1,3-enynes in good to high yields was described recently by Collins[81] using cobalt catalysis and **PS-I** (Scheme 18, B). Remarkably, it was possible to apply the reaction to macrocyclic hydroalkynylations, a class of motive present in natural products. The mechanistic interpretation of the obtained results is slightly different from the other discussed examples with cobalt. In this case the SET event was carried out by the photosensitizer in its excited state. The *PS was supposed to be able to reduce, in a consecutive manner, the LCo(II) (L= chelating phosphine) to the LCo(0) complex. Insertion of the alkyne gave an intermediate LCo(II)H(C≡CR) complex. This complex was then involved in a migratory insertion, resulting in the formation of an ene-ine Co(II)H. Oxidation of this complex to a new LCo(III)H(ene-ine) was proposed to occur via SET from the oxidized photosensitizer $PS^{\bullet+}$. At this point, a reductive elimination forms a LCo(I) complex, that re-enters in the catalytic cycle, and the observed product is formed. Since DIPEA is necessary for the reaction, the authors suggested that the sacrificial amine is involved in the restoration of the PS from the $PS^{\bullet+}$ oxidized state.

5.3 Reactions promoted by acridinium.

Lei and co-workers reported a dual cobalt $[Co(dmgH)(dmgH_2)]Cl_2$ photoredox approach to phosphorylated products in the presence of acridinium **PS-VIII** as photosensitizer (Scheme 19, A).[82] The high oxidative ability of acridinium in its excited state is necessary, as other tested organic photosensitizers were unable to promote the reaction. Mechanistically, the reaction is initiated by the oxidation of the organic electron-rich aromatic substrates employed **66**, leading to the corresponding radical cation due to *PS. Then $P(OR)_3$ **67** acts as a nucleophile and the so-formed radical is reduced by Co(III) to the arenium, forming a Co(II) species. Aromatization with loss of a proton and elimination of ethyl group gave the observed product **68**. The $PS^{\bullet-}$, formed during the oxidation of the aromatic substrate, is the strong reductant responsible for the formation of Co(I) from Co(II). The cobalt in low oxidation state is able to intercept the proton to give a Co(III)H intermediate. Cobalt hydride promotes the formation of the aromatic phosphonium salt, since it reacts with H^+ with consequent irreversible formation of H_2.

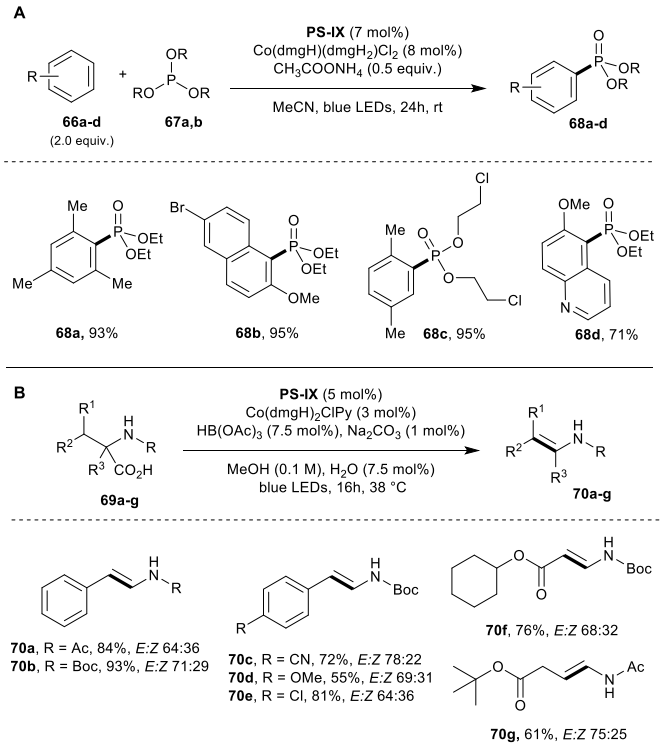

Scheme 19. (A) External oxidant-free oxidative phosphorylation of $C(sp^2)$–H bonds by merging visible-light photoredox with cobalt catalysis; (B) Photoredox/cobaloxime dual catalytic decarboxylative elimination for the synthesis of enamides and enecarbamates.[82,83]

Enamides and enecarbamates **70** were directly obtained from *N*-acyl amino acids **69** by using a dual photoredox strategy that comprises cobalt catalysis (Scheme 19, B).[83] The catalytic cycle can be explained considering an initial oxidation of the carboxylate anion promoted by the photoexcited acridinium, followed by decarboxylation. The so-formed alkyl radical is trapped by the Co(II) complex (cobaloxime) to form a Co(III)alkyl, that through HAT is furnishing CoIII hydride and the desired alkene. The HAT event forms a Co(III)H hydride, that is responsible for the deprotonation of carboxylate followed by H_2 evolution. Since Co(III) returns in the cycle, a reduction step is needed, probably due to the $PS^{\bullet-}$, allowing the closure of both the Co and photo-catalytic cycles.

6. Organic dyes in photoredox palladium mediated processes.

The first report employing a palladium cycle and a photocatalytic cycle was described by Osawa with a variation of Sonogashira coupling reaction. The reaction proceeded in absence of copper,[84] using $[Ru(bpy)_3Cl_2]$ as photosensitizer, that considerably improved the result of the cross coupling. The authors were well aware of the possibilities offered by the potential of $*[Ru(bpy)_3Cl_2]$ employed and pointed out the possibility to set up new multicomponent catalysis. However, only some years later, with the examples of metallaphotoredox catalysis with palladium described by Sanford,[13] the design of catalytic cycles, with the selection of adapted photosensitizer for the SET event, was recognized. The work was about C–H arylation of aryl pyridines. The PS ($[Ru(bpy)_3]^{2+}$) in its excited state was able to perform the reduction of the aryldiazonium salts to produce aryl radicals. At the same

time, the oxidized form of the photosensitizer, $PS^{\bullet+}$ (generated in the first SET event) is able to perform the required oxidation of the intermediate Pd(III) arylmetallacycle to the Pd(IV) derivative, leading to the desired product via reductive elimination.

6.1 Reactions promoted by 9,10-dihydroacridine.

Similarly to what was reported by Sanford,[13] Xu and co-workers have described the preparation of arylated pyridine products via dual photoredox catalysis using, instead of $[Ru(bpy)_3]^{2+}$, the 9,10-dihydroacridine (**PS-XII**, Figure 5) as competent organic photoredox catalyst, under mild conditions at room temperature (Scheme 20, A).[85] The mechanistic picture follows the proposal of Sanford, with the photoexcited *[**PS-XII**] able to generate the aryl radical that is intercepted by the Pd(II) palladacycle to give the Pd(III) intermediate. Oxidation of the Pd(III) and reductive elimination gave the observed product (**74** and **75**).

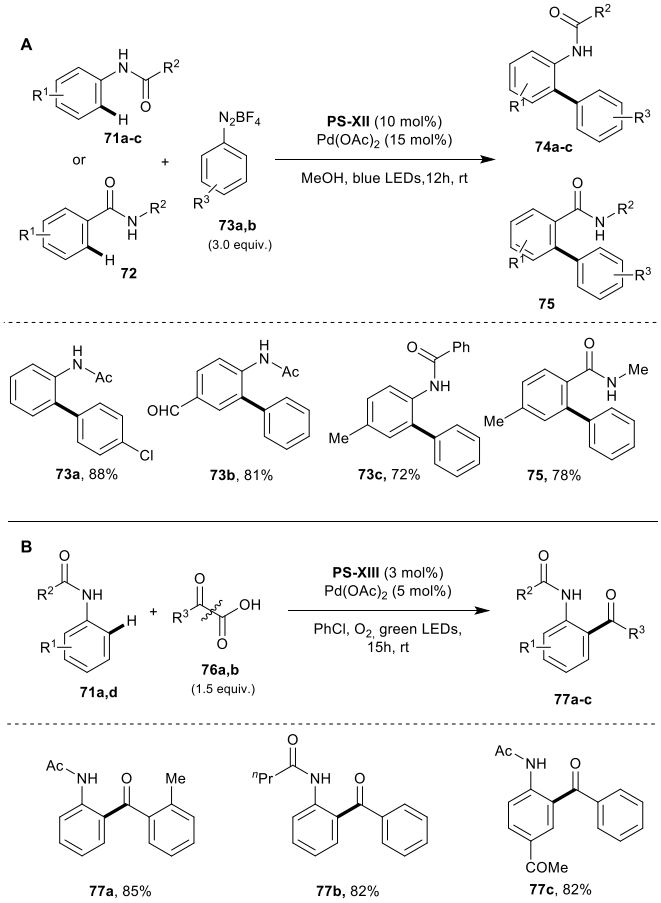

Scheme 20. (A) Dual Pd/photoredox catalytic system for the C(sp^2)–H arylation of arenes with aryldiazonium salts; (B) Dual Pd/Eosin Y photoredox catalytic system for *ortho*-acylation of acetanilides with α-oxocarboxylic acids.[85,86]

6.2 Reactions promoted by Eosin.

In 2015, Wang and co-workers reported the first example of the possibility to use organic dyes in conjunction with metallaphotoredox catalysis.[86] They described the acylation of acetanilides **71** via a C–H functionalization (Scheme 20, B). In the mechanistic picture, phenylglyoxylic acid is oxidized by Eosin Y (**PS-XIII**, Figure 6) to the corresponding acyl radical, while the photosensitizer is transformed into the $PS^{\bullet-}$ form. $PS^{\bullet-}$ is restored to Eosin by reaction with molecular oxygen, which in turns is reduced to superoxo radical $O_2^{\bullet-}$. The catalytic cycle with palladium is a well-known directed assisted metalation that forms a palladacycle ArPd(II)(OAc). The palladacycle intercepts the acyl radical giving the ArPd(OAc)(III)COPh, that is oxidized by $O_2^{\bullet-}$ to the Pd(IV) intermediate. Reductive elimination leads to the formation of the isolated compounds **77**.

6.3 Reactions promoted by 4CzIPN.

Decarboxylative formylation of aryl and heteroaryl halides with glyoxylic acid **78** was performed by means of synergistic catalysis using an organic dye, **PS-I** (Figure 3), and phosphine (**L7**, Scheme 18, A) as ligand (Scheme 21, A).[87] The reaction featured a broad scope for aryl and heteroaryl halides and allowed the synthesis of functionalized aryl and heteroaryl aldehydes **79**. For the rationale of the reaction, the author proposed a reductive quenching of the **PS-I**, with the formation of a $PS^{\bullet-}$ able to reduce the intermediate Pd(III)Aryl(acyl)Br derivative to the Pd(II) complex. The latter, upon reductive elimination, leads to the formylated products.

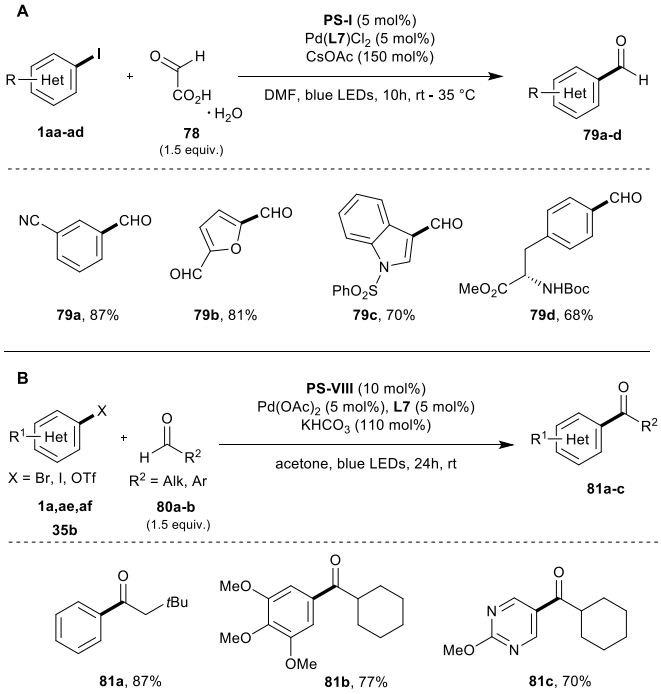

Scheme 21. (A) Organophotoredox/palladium co-catalyzed decarboxylative formylation of iodoarene using glyoxylic acid monohydrate; (B) Merging HAT photocatalysis with Pd catalysis for C(sp^2)−H arylation and alkenylations of aldehyde.[87,88]

6.4 Reactions promoted by anthraquinone.

Zheng and co-workers reported the use of an interesting combination for palladium.[88] With the idea to build up a process to prepare ketones **81**, they have used palladium chemistry in the presence of anthraquinone **PS-VII** (Figure 4) as photosensitizer (Scheme 21, B). The authors, on the basis of DFT calculations, suggested a Pd(0)−Pd(II)−Pd(III)−Pd(I)−Pd(0) pathway. The abstraction of the hydrogen from an aldehyde is determined by the excited anthraquinone (***PS-VIII**), with the generation of an anthraquinone radical (**PS-VIII**$^{\bullet-}$). The calculation was also able to explain the need of bases ($KHCO_3$). By studying the reaction profile, authors found that the base abstracts a Br atom from the Pd(I)−Br complex and a proton from AQ-H radical in a concerted manner. This step regenerates the Pd(0) catalyst. The Pd(0) surrounded by the ligand reacts with aryl bromide in the usual manner (i.e. oxidative addition), leading to ArPd(II)Br. This intermediate is intercepted by the acyl radical produced by H abstraction, forming the Pd(III)AcylArBr intermediate, that, through reductive elimination, furnished the observed organic product, with concomitant formation of LPd(I)Br. The concerted elimination/deprotonation of the AQ-H radical closes the catalytic cycle.

7. Organic dyes in photoredox copper mediated processes.

Copper has been under active investigations for photoredox application from several points of view.[18] Copper can be used for the preparation of quite effective and tunable photocatalysts. The employment of chiral ligands (in particular BOX ligands) allowed the possibility to use the photoredox catalyst in metal mediated processes producing effective stereoinduction. In addition, the control of the supposed Cu(I)/Cu(III) catalytic cycle for effective cross coupling can be realized through the synergistic applications of suitable photosensitizers and copper complexes. Furthermore, copper complexes are also photoactive compounds, able to reach excited states, and these properties can be advantageously introduced to control copper mediated reactions. Many photochemical cross-coupling reactions able to form C–C, C–N, C–O, and C–S bonds have been developed in recent years.[89] However, application of organic dyes to copper catalytic metallaphotoredox reactions is still limited.

7.1 Reactions promoted by rose Bengal.

Fu and coworkers reported an example of alkynylation of tetrahydroisoquinolines, promoting the photoredox reaction with Rose Bengal (**PS-IX**, Figure 6). In deep analysis, this is not a synergistic metallaphotoredox reaction, since rose Bengal is able, though the photoredox cycle, to oxidize the tetrahydroisoquinolines to the reactive imine.[90] Then, the imine reacts with the nucleophilic copper acetylide obtained in situ, affording the alkynylated isoquinoline derivative.

7.2 Reactions promoted by Eosin.

An *ortho*-C–H trifluoromethylation of aniline derivatives **71** using the commercially available CF_3SO_2Na as source of CF_3 (Scheme 22, A), in the presence of $(NH_4)_2S_2O_8$ was reported.[91] In the mechanistic analysis, the authors proposed a dual copper/photoredox mechanism. Eosin Y (**PS-XIII**, Figure 6) in its excited state is oxidized to $PS^{\bullet+}$ by the sacrificial reagent $(NH_4)_2S_2O_8$, and $SO_4^{\bullet-}$ is formed. This radical species is responsible for the formation of CF_3 radical. Copper(II) intercepts the radical CF_3 giving a $Cu(III)CF_3$ complex. According to the authors, $PS^{\bullet+}$ is able to oxidize the anilide to the corresponding aryl radical, which in turn interacts with the $Cu(III)CF_3$. The authors proposed an oxidation of the aryl radical to anilide arenium ion, followed by a direct nucleophilic reaction between CF_3 coordinated to copper and the carbenium ion, to give the observed product **83**.

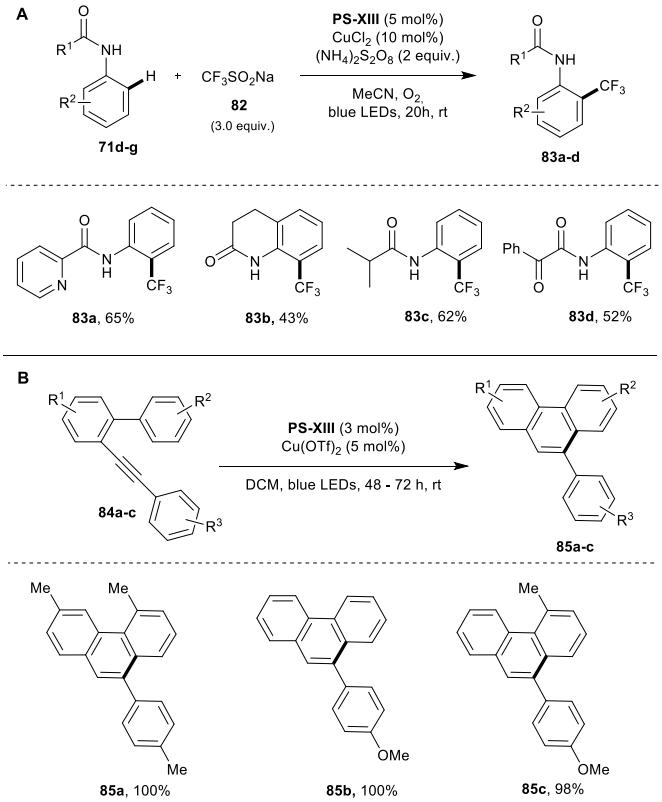

Scheme 22. (A) Copper/photoredox dual catalytic system for *ortho*-C–H trifluoromethylation of aniline derivatives; (B) C–C triple bond activation by merging photoredox and Lewis acid copper catalysis for the cyclization of arene-ynes.[91,93]

In a quite similar mechanism, a dual copper-promoted perfluoroalkylation of benzamides was described through the assistance of 8-aminoquinoline as directing group.[92] The cyclometalated Cu(II) species, arisen from C–H activation step, reacts with the perfluoroalkyl radicals to give a Cu(III) complex, that generates the product via reductive elimination. In this example, the perfluoroalkyl radical is directly obtained by oxidative quenching of the *PS excited state to give $PS^{\bullet+}$ able to oxidize Cu(I) to its reactive form. Polycyclic structures can be obtained by copper mediated cyclization in the presence of organic photosensitizer. In particular, Guo reported the synthesis of phenanthrene derivatives **85** (Scheme 22, B).[93] The authors proposed that copper could interact with alkynes **84** as π-acid, followed by oxidation of this complex by the excited state of the photocatalyst, to afford the corresponding Cu(III) intermediate. The highly electrophilic Cu(III) can help in promoting the subsequent internal Friedel-Crafts reactions, that is followed by re-aromatization. The phenanthrylcopper(III) complex is reduced to Cu(II) by $PS^{\bullet-}$ state, and after a protonation of copper complex, copper(II) is regenerated to restart the cycle.

7.3 Reactions promoted by *N*,*N*-diaryl-dihydrophenazines.

A dual organophotoredox/copper catalytic methodology for the preparation of alkenes, via decarboxylative olefination processes, was recently described by Glorius (Scheme 23).[94] Kinetic experiments performed on initial rate of the reaction suggested that the electron transfer from the photoexcited state of the catalyst is the turnover limiting step. The *N*,*N*-diaryl-dihydrophenazine (**PS-XVI**, Figure 7) PS is a strong reductant in its excited state (E(PS•+/*PS)= −1.80 V vs. SCE), and is able to reduce the RAE (redox active ester) derivative, to give the corresponding radical after fragmentation.[6,95] The formed radical is trapped by Cu(II), forming a Cu(III)alkyl derivative that gives, via an oxidative elimination, the alkene. Copper(I) formed by this elimination is oxidized by the PS•+ state of the catalyst.

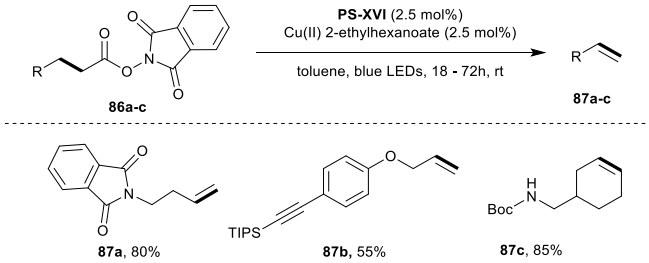

Scheme 23. Dual organophotoredox/copper catalyzed decarboxylative olefination of activated aliphatic acids.[94]

7.4 Reactions promoted by acridinium.

In another example of metallaphotoredox catalysis based on copper, Xia and co-workers[96] reported the formation of quinoline, via acridinium catalysis (Scheme 24). Acridinium (**PS-IX**) is able to oxidize the amine to the corresponding amine radical, in equilibrium with the C-centered radical. This radical then reacts with the alkyne giving the quinoline radical. The latter is trapped by dioxygen, present in the reaction. Copper is involved in the reduction of the peroxyl radical formed, providing the isolated quinoline derivative **89**.

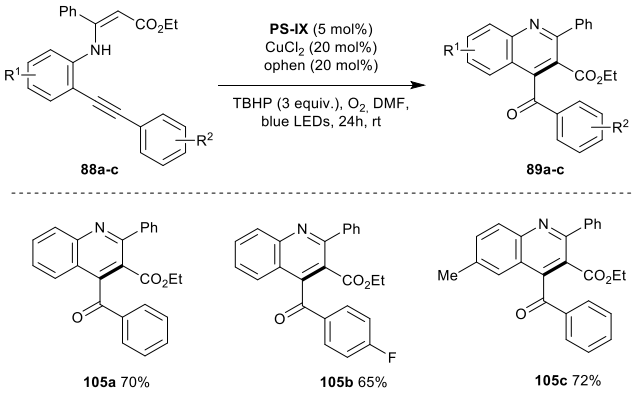

Scheme 24. Dual organophotoredox/Copper catalyzed oxidative cyclization of aromatic enamines for the synthesis of quinoline derivatives.[96]

Larionov and co-workers[97] have recently described an efficient and selective C–N bond-forming reactions with a dual catalytic system for *N*-alkylation of diverse aromatic carbocyclic and heterocyclic amines with carboxylic acids. The reaction that is enabled by avisible light in the presence of acridine, and copper(II) complexes ($Cu(hfac)_2$ hfac = 1,1,1,5,5,5-hexafluoropentane-2,4-dione). EPR studies indicated that a complex that the aromatic amine is coordinated to copper(II), with a stoichiometry 1:1. The photocatalyst induced a decarboxylation with concomitant formation of a radical specie intercepted by the copper-aniline complex, to give a Cu(III) intermediate. The reductive elimination from this intermediate gave copper(I) and the observed alkylated aniline derivative.

8. Organic dyes in photoredox with other metals: iron, gold, chromium, titanium, bismuth and cerium.

8.1 Iron dual catalysis with organic dyes.

The renewed interest in the application of iron complexes in catalysis is testified by a recent review reporting more than 1500 references.[98] Iron is cheap, abundant and presents low toxicity. Therefore, the merging of dual photoredox catalysis with iron complexes is now under scrutiny. Only few examples in which organic dyes are employed in combination with iron catalysis have been reported in literature. The first example concerns an important application of a dual photoredox system for the activation of CO_2. Robert discovered[99] that the $8e^-/8H^+$ reduction of CO_2 to CH_4 was possible by employing a dual catalytic approach that

combined an iron porphyrin catalyst with an iridium-based photosensitizer [*fac*-Ir(ppy)$_3$] (ppy = 2-phenylpyridine). In order to replace the expensive Ir(III) photocatalyst with an organic dye, Robert and Miyake reported the possibility of using phenoxazine-based organic photosensitizers.[100] Upon deep investigation of the mechanism, the authors proposed that the iron porphyrin is reduced to the lower oxidation state of Fe(0). All the reduction potentials of the Fe-complex, E(Fe(III)/Fe(II)), E(Fe(II)/Fe(I)) and E(Fe(I)/Fe(0)), are less negative compared to the excited state oxidation potential of the organic dye (E(PS$^{\bullet+}$/*PS)= ca. −1.78 V vs. SCE). The interaction between the excited state of the photocatalyst and the iron complex was proven by means of Stern-Volmer analysis. The Fe(0) species interacts with CO_2, and the resultant Fe(II)CO_2 complex then gives Fe(II)CO after protonation and liberation of water. This intermediate is further reduced and protonated to from methane. Chakraborty and Von Wangelin have recently reported the combination of visible-light photocatalysis promoted by an organic dye with inexpensive and available $FeCl_2$ for an iron-catalysed cyclotrimerization of alkynes (Scheme 25).[101]

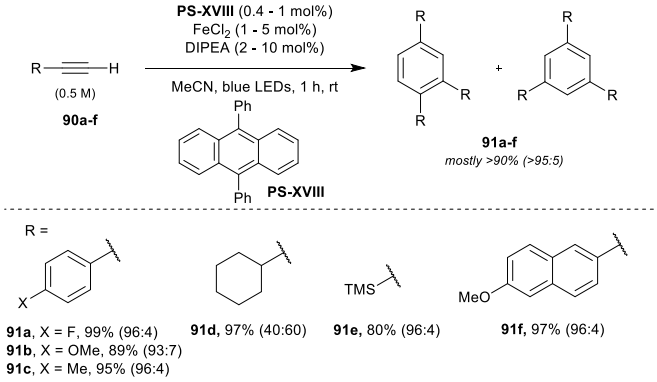

Scheme 25. Dual organophotoredox/Iron catalyzed cyclotrimerization of alkynes.[101]

9,10-diphenylanthracene (**PS-XVIII**) was used as the photosensitizer in the investigation. On the basis of a careful mechanistic investigation, the authors proposed that the PS in its excited state is reductively quenched by DIPEA, reaching a PS$^{\bullet-}$ state that is a strong reductant (E(PS/PS$^{\bullet-}$) = –1.9 V vs. SCE). PS$^{\bullet-}$ then reduces iron to its low oxidation state, and the cluster of reduced iron is able to trimerize the alkyne.

8.2 Gold dual catalysis with organic dyes.

π-Lewis acidic gold complexes have been extensively studied for the activation of substrates followed by nucleophilic addition. In most of these reactions, gold maintains (I) oxidation state. In order to take advantage of the catalytic cycle Au(I)/Au(III) and incorporate π-activation events with oxidative additions/reductive elimination, normally, stoichiometric powerful oxidants need to be employed. The merging of photoredox and gold catalysis has been accomplished by Glorius.[19] By incorporation of radical cycles in the framework of gold catalysis, he was able to expand the repertoire of gold mediated transformations.[102] Quite recently, an innovative carbenium photocatalyst (E(*PS/PS$^{\bullet-}$)= +1.15 V vs. SCE in MeCN)[103] was used to replace [Ru(bpy)$_3$](PF_6)$_2$ in Glorius's dual gold/photoredox-catalyzed C(sp)−H arylation of terminal alkynes **90c** (Scheme 26).[104]

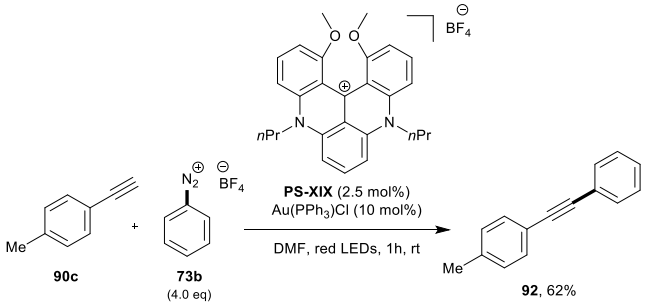

Scheme 26. Dual Au/photoredox-catalyzed C(sp)−H arylation.

Remarkably, the organic photocatalyst is able to perform this catalysis under red light irradiation. In the proposed catalytic cycle, PS is able to form the aryl radical by reduction of the diazonium salt **73b**, that is added to the [Ph_3PAu(I)alkyne] complex, leading to Au(II) intermediates. After oxidation to Au(III), carried out by PS$^{\bullet+}$, reductive elimination gives the observed product **92**.

8.3 Chromium dual catalysis with organic dyes.

Chromium is considered a suspicious element, both toxic and dangerous. Therefore, its use in organic synthesis is avoided. Yet, recent publications remarked the low toxicity of chromium(II) and (III).[105] Chromium is used to promote effective variants of Nozaki-Hiyama-Kishi (NHK) reactions at an industrial scale.[106] However, a stoichiometric use of a reducing metal and additives is necessary for the catalytic use of chromium, thus producing waste and by-products. Photoredox catalysis could be a possible solution to avoid metals as reductant and to use light to promote the NHK reaction. A remarkable example of a photoredox NHK reaction based upon a C–H functionalization, was recently reported by Glorius.[107] The reaction is based on the formation of allylradicals from alkenes by photoredox catalysis. These radicals interact with Cr(II) to give the nucleophilic allylating Cr(III) species. The described reaction employed the iridium complex ($[Ir(dF(CF_3)ppy)_2(dtbbpy)][PF_6]$ as photocatalyst. Since the reaction formed the allyl radical by reductive quenching of [Ir(III)] photocatalyst, allyl(hetero)arenes are suitable substrates for this transformation, due to their oxidation potential. The addition of the allyl Cr(II) species to aldehyde gave the desired products with good diastereoselection, controlled by a Zimmerman-Traxler transition state.

Kanai and co-workers reported an enantioselective version of the reaction featuring the employment of chiral BOX ligands (**L9**) and acridinium salt as photocatalyst **PS-IX** (Scheme 27, A).[108] The use of a stronger photooxidant allowed the employment of simple alkenes **93** as starting material. Broad functional group tolerance and the possibility of utilizing aliphatic and aromatic aldehydes **80** as electrophiles make these reactions interesting. Quite recently, additional work was published in this area of research. Glorius reported a regioselective, diastereoselective, and enantioselective three-component dialkylation of substituted dienes **95** with 4-alkyl-1,4-dihydropyridines **6** and aldehydes **115**, for the synthesis of homoallylic alcohols **95** (Scheme 27, B).[109] The organic photocatalyst employed in the reaction is 4CzIPN (**PS-I**) which, once in its excited state, is reduced by the dihydropyridine derivatives ($E(^*PS/PS^{\bullet-})$= +1.35 V vs. SCE) in MeCN; $E(DHP^{\bullet+}/DHP)$= +1.10 V vs. SCE in MeCN). $PS^{\bullet-}$ is then able to reduce chromium (E(Cr(III)/Cr(II)= −0.51 V vs. SCE in dimethylformamide). The addition of radical formed by fragmentation of oxidized dihydropyridine derivatives occurred to the diene, and the so-formed allyl radical is trapped by Cr(II), giving the corresponding allylCr(III) chromium reagent. As in the reaction described by Kanai, the enantioselective variant of the reaction is carried out with BOX ligands.

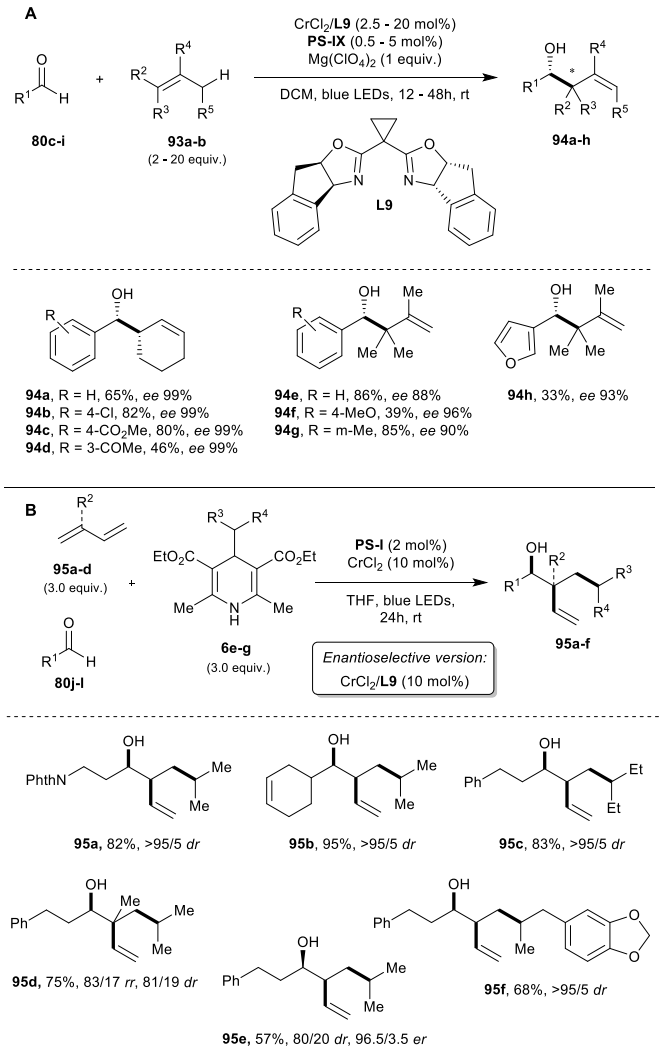

Scheme 27. (A) Catalytic asymmetric allylation of aldehydes with alkenes via allylic C(sp^3)–H functionalization mediated by dual organophotoredox and chiral chromium catalysis (B) Selective three-component dialkylation of 1,3-dienes with alkyl Hantzsch esters and aldehydes enabled by dual photoredox and chromium catalysis.[108,109]

Kanai reported an improvement as far as the applicability of the photoredox NHK reaction to synthetic problems is concerned.[110] Using a photoredox cycle with acridinium **PS-IX** in the presence of a hydrogen-atom-transfer catalyst (**CAT2**), Kanai was able to use various alkenes **93**, and in particular, butene as substrate (Scheme 28).

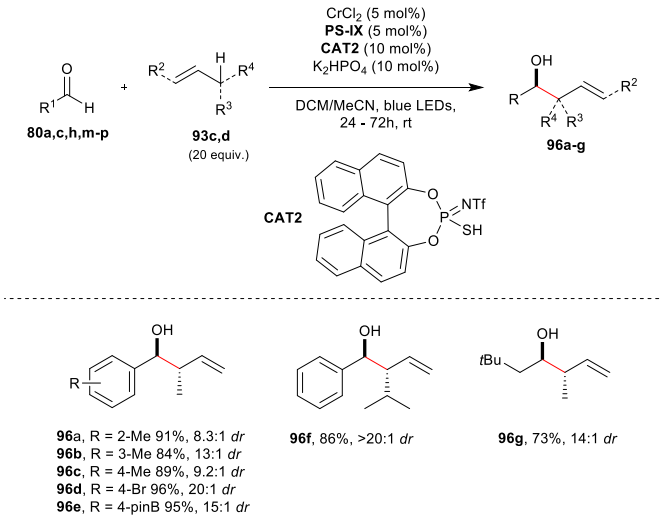

Scheme 28. Ternary hybrid catalyst system comprising a photoredox catalyst, a HAT catalyst, and a chromium complex catalyst, enabling catalytic allylation of aldehydes with alkenes.[109]

Ketyl radicals seem not to be involved in the reaction and deuteration experiments pointed out that a HAT event carried out by the sulfur HAT catalysis is involved. The thiophosphoric imide **HAT-PS2** catalyst was designed on the basis of other studies and on the basis of BDE of allylic bonds (85 Kcal/mol) compared to the BDE of the catalyst (ca. 87 kcal/mol). Simple diastereoselection of the reaction is quite high and heterosubstituted alkene are also reactive. Enantiomeric excesses of the reaction are still under 90%, but improvements could be possible.

8.4. Titanium dual catalysis with organic dyes.

Titanium is one of the most abundant and environmentally friendly metal. The radical chemistry of titanium in low oxidation state has been exploited in the past years.[111] In titanium-catalyzed applications, as in the case of chromium, a metal acting as stoichiometric reductant (Zn or Mn) and additives were necessary[112] To solve these issues, the combination of titanium catalytic cycles with photoredox catalysis could be the solution.[24] Recently, Gansäuer reported a leading example of formation and use of Ti(III) using photoredox catalysis with polypyridyl complexes (either Ir(III) or Ru(II)) as photosensitizers). $Cp_2Ti(III)Cl$ was generated by reduction of $Cp_2Ti(IV)Cl_2$ through photoredox processes in the presence a sacrificial hydrogen-atom donor (Hantzsch ester **HE**; $E(HE^{\bullet+}/HE)$ = +1.0 V vs. SCE) and the reaction with epoxides was explored.[113] In a very similar reactivity, Shi and coworkers[114] used 4CzIPN **PS-I** for the synthesis of spirocyclic compounds **99** and **100** (Scheme 29, A).

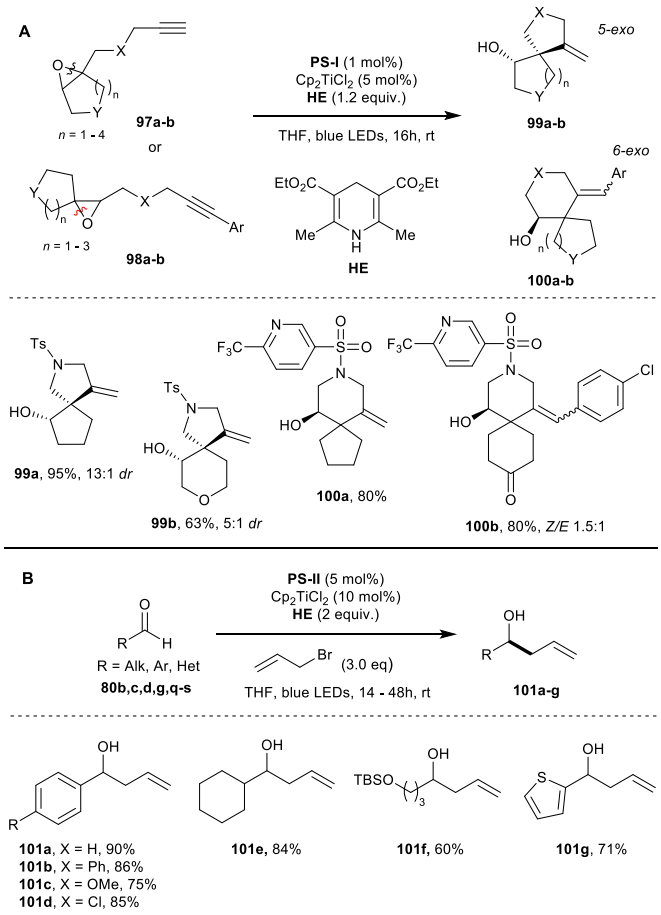

Scheme 29. (A) Synergistic titanocene/photoredox dual catalysis for the radical opening/spirocyclization of epoxyalkynes; (B) Dual photoredox/titanium-catalyzed allylation of aldehydes.[114,115]

The reaction occurred by the direct reduction of $Cp_2Ti(IV)Cl_2$ by the organic photosensitizer, with the $Cp_2Ti(III)Cl$ able to open the epoxide and form a C-centered radical, that triggered the cyclization process. The final radical obtained was intercepted by the H-donor, **HE**. Authors have unfortunately carried out the pertinent photophysical studies on $[Ir(ppy)_2(dtbbpy)]PF_6$, due to the difficulties related to the Cp_2TiCl_2 absorption. Gualandi, Bergamini, and Cozzi have recently reported a Barbier-type photoredox allylation reaction mediated by Cp_2TiCl_2 using TADF dye 3DPAFIPN **PS-II** (Scheme 29, B).[115] Full photophysical details of the reaction were clarified and in the proposed mechanism the organic photocatalyst was proved to be able to reduce Ti(IV) to Ti(III). Allylbromo derivatives were used, instead of alkenes. The consecutive reaction of allyl derivatives with the two reduced titanium molecules, as suggested in titanium Barbier mediated reactions,[116] forms the active nucleophilic titanium reagent.

8.5. Bismuth dual catalysis with organic dyes.

Bismuth is a safe and inexpensive metal, and has been used in allylation reactions[117] in the presence of stoichiometric metals as reductant, such as Al, Mg, Fe and Zn[118] or $NaBH_4$.[119] Gualandi and Cozzi have recently explored the possibility of replacing these reducing agents with a photoredox catalytic cycle (Scheme 30).[120] Allylation of aromatic and aliphatic aldehydes with allyl bromide was possible by the use of catalytic amount of $Bi(OTf)_3$ in the presence of Hantzsch's ester as the sacrificial reductant and dicyanobenzene photocatalyst 3CzClIPN (**PS-III**). The reaction proceeds under mild reaction conditions, tolerance of oxygen, and in aqueous solvent. These characteristics make this photoredox methodology attractive for green and sustainable synthesis of homoallylic alcohols.

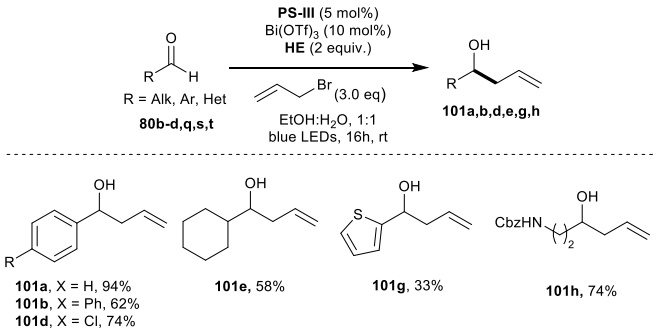

Scheme 30. Dual photoredox/bismuth-catalyzed allylation of aldehydes.[120]

8.6. Cerium dual catalysis with organic dyes.

Abundant and inexpensive cerium(IV) can participate in redox reactions by LMCT states of its complexes.[121] On the basis of this report, Zhuo and co-workers have used the properties of cerium to generate alkoxy radicals from alcohols through a coordination−LMCT−homolysis process.[122] More recently, Zhuo has reported an interesting combination between cerium photocatalysis and photoinduced electron transfer by an organic dye that is capable of ring expansion of available cycloalkanols, to access bridged lactones (scheme 31).[123]

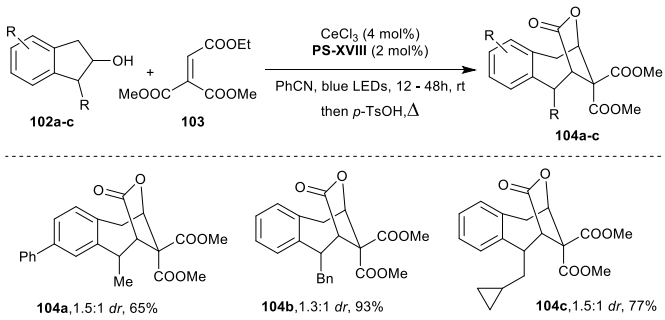

Scheme 31. Dual cycloaddition of alkanols promoted by cerium[123]

The dual cycloaddition is promoted by coordination of the cycloalkanols to cerium complex and, photoexcitation produces an alkoxy radical, that decompose to a nucleophilic alkyl radical. The produced alkyl radical is capable to react with the alkene, forming a new C−C bond and an α-acyl radical. This α-acyl radical ($E_{1/2}$ = −0.60 V is getting reduced by the strongly reducing photoexcited state of the PC ($E_{1/2}$ = −1.77 V versus SCE in MECN).

Conclusions

In conclusion, application of organic dyes in metallaphotoredox catalysis is still an area that deserves better investigation and efforts. Many reactions promoted by expensive and rare Ru(II) and Ir(III) reactions can be effectively catalyzed using suitable organic dyes. Reviews and recent articles have properly assessed the photophysical properties of these dyes, facilitating a good selection and trials. In addition, several dyes are easily accessible, allowing fine tuning of their properties for more sophisticate employment. The interesting class of TADF dyes, comprising hundreds of molecules, has been investigated with only very few molecules. We believe that the association of organic dyes with metal mediated processes will attract more investigations and interesting applications in the future. Moreover, the possibility of reaching quite high reductive or oxidative excited states with multiple photons excitements, can further improve the possibilities offered by organic dyes, in more challenging and not yet explored applications, such as activation of small molecules (N_2) or the catalytic use of low valent metals.

Conflicts of interest

There are no conflicts to declare.

Acknowledgements

National PRIN 2017 project (ID: 20174SYJAF, SURSUMCAT) are acknowledged for financial support of this research.

Notes and references

1) For selected reviews on photoredox catalysis, see: (a) F. Khan, R. S. Tare, R. O. C. Oreffo and M. Bradley, *Angew. Chem. Int. Ed.*, 2009, **48**, 978–982; (b) T. P. Yoon, M. A. Ischay and J. Du, *Nat. Chem.*, 2010, **2**, 527–532; (c) J. M. R. Narayanam and C. R. J. Stephenson, *Chem. Soc. Rev.*, 2011, **40**, 102–113.; (d) J. Xuan and W. J. Xiao, *Angew. Chem. Int. Ed.*, 2012, **51**, 6828–6838; (e) L. Shi and W. Xia, *Chem. Soc. Rev.*, 2012, **41**, 7687–7697; (f) D. Ravelli and M. Fagnoni, *ChemCatChem*, 2012, **4**, 169–171; (g) C. K. Prier, D. A. Rankic and D. W. C. MacMillan, *Chem. Rev.*, 2013, **113**, 5322–5363; (h) L. Marzo, S. K. Pagire, O. Reiser and B. König, *Angew. Chem. Int. Ed.*, 2018, **57**, 10034–10072; (i) R. C. McAtee, E. J. McClain and C. R. J. Stephenson, *Trends Chem.*, 2019, **1**, 111–125.
2) Modern Molecular Photochemistry of Organic Molecules, Turro, N. J.; Ramurthy, V.; Scaiano, J. C. 2010, University Science Books, Sausalito, California.
3) Photochemistry and Photophysics: Concepts, Research, Applications, V. Balzani, P. Ceroni, A. Juris, Wiley 2014.
4) S. Mai and L. González, *Angew. Chem. Int. Ed.*, 2020, **59**, 16832–16846.
5) Photochemistry and Photophysic of coordination compounds, Balzani, V.; Campagna, S. Springer, 2007.
6) K. Okada, K. Okamoto, N. Morita, K. Okubo and M. Oda, *J. Am. Chem. Soc.*, 1991, **113**, 9401–9402.
7) C. B. Larsen and O. S. Wenger, *Chem. Eur. J.*, 2018, **24**, 2039–2058.
8) (a) A. Gualandi, M. Marchini, L. Mengozzi, H. T. Kidanu, A. Franc, P. Ceroni and P. G. Cozzi, *Eur. J. Org. Chem.*, 2020, **2020**, 1486–1490; (b) A. Gualandi, M. Marchini, L. Mengozzi, M. Natali, M. Lucarini, P. Ceroni and P. G. Cozzi, *ACS Catal.*, 2015, **5**, 5927–5931.
9) J. Twilton, M. Christensen, D. A. DiRocco, R. T. Ruck, I. W. Davies and D. W. C. MacMillan, *Angew. Chem. Int. Ed.*, 2018, **130**, 5467–5471.
10) C. Wu, N. Corrigan, C. H. Lim, K. Jung, J. Zhu, G. Miyake, J. Xu and C. Boyer, *Macromolecules*, 2019, **52**, 236–248.
11) (a) A. Gualandi, A. Nenov, M. Marchini, G. Rodeghiero, I. Conti, E. Paltanin, M. Balletti, P. Ceroni, M. Garavelli and P. G. Cozzi, *ChemCatChem*, 2021, **13**, 981-989; (b) S. M. Sartor, C. H. Chrisman, R. M. Pearson, G. M. Miyake and N. H. Damrauer, *J. Phys. Chem. A*, 2020, **124**, 817–823.
12) N. A. Romero and D. A. Nicewicz, *Chem. Rev.*, 2016, **116**, 10075–10166.
13) D. Kalyani, K. B. McMurtrey, S. R. Neufeldt and M. S. Sanford, *J. Am. Chem. Soc.*, 2011, **133**, 18566–18569.
14) Z. Zuo, D. T. Ahneman, L. Chu, J. A. Terrett, A. G. Doyle and D. W. C. MacMillan, *Science*, 2014, **345**, 437–440.
15) J. C. Tellis, D. N. Primer and G. A. Molander, *Science*, 2014, **345**, 433–436.
16) J. Twilton, C. C. Le, P. Zhang, M. H. Shaw, R. W. Evans and D. W. C. MacMillan, *Nat. Rev. Chem.*, 2017, **1**, 0052.
17) R. Sun, Y. Qin and D. G. Nocera, *Angew. Chem. Int. Ed.*, 2020, **59**, 9527–9533.
18) A. Hossain, A. Bhattacharyya and O. Reiser, *Science*, 2019, **364**, eaav9713.
19) M. N. Hopkinson, A. Tlahuext-Aca and F. Glorius, *Acc. Chem. Res.*, 2016, **49**, 2261–2272.
20) P. Chuentragool, D. Kurandina and V. Gevorgyan, *Angew. Chem. Int. Ed.*, 2019, **58**, 11586–11598.
21) D. C. Fabry and M. Rueping, *Acc. Chem. Res.*, 2016, **49**, 1969–1979.
22) D. C. Fabry, M. A. Ronge, J. Zoller and M. Rueping, *Angew. Chem. Int. Ed.*, 2015, **54**, 2801–2805.
23) J. Zhang, D. Campolo, F. Dumur, P. Xiao, J. P. Fouassier, D. Gigmes and J. Lalevée, *ChemCatChem*, 2016, **8**, 2227–2233.
24) A. Fermi, A. Gualandi, G. Bergamini and P. G. Cozzi, *Eur. J. Org. Chem.*, 2020, **2020**, 6955–6965.
25) Q. Q. Zhou, Y. Q. Zou, L. Q. Lu and W. J. Xiao, *Angew. Chem. Int. Ed.*, 2018, **58**, 1586–1604.
26) H. Uoyama, K. Goushi, K. Shizu, H. Nomura and C. Adachi, *Nature*, 2012, **492**, 234–240.
27) E. Speckmeier, T. G. Fischer and K. Zeitler, *J. Am. Chem. Soc.*, 2018, **140**, 15353–15365.
28) G. Porter and P. Suppan, *Trans. Faraday Soc.*, 1965, **61**, 1664–1673.
29) Handbook of Photochemistry, Montalti, M., Credi, A., Prodi, L., and Gandolfi, M.T., Taylor & Francis Group, 2006.
30) Y. Shen, Y. Gu and R. Martin, *J. Am. Chem. Soc.*, 2018, **140**, 12200–12209.
31) K. Mishiro, T. Kimura, T. Furuyama and M. Kunishima, *Org. Lett.*, 2019, **21**, 4101–4105.
32) A. Benniston, A. Harriman, P. Li, J. Rostron, H. Van Ramesdonk, M. Groeneveld, H. Zhang and J. Verhoeven, *J. Am. Chem. Soc.*, 2005, **127**, 46, 16054–16064.
33) I. A. MacKenzie, L. Wang, N. P. R. Onuska, O. F. Williams, K. Begam, A. M. Moran, B. D. Dunietz and D. A. Nicewicz, *Nature*, 2020, **580**, 76–80, and ref. therein.
34) K. Fidaly, C. Ceballos, A. Falguières, M. Sylla-Iyarreta Veitia, A. Guy and C. Ferroud, *Green Chem.*, 2012,**14**, 1293–1297.
35) H. E. Lessing, D. Richardt, and A. Von Jena, *J. Mol. Struct.*, 1982, **84**, 281–292.
36) X. F. Zhang, I. Zhang and L. Liu, *Photochem. Photobiol.*, 2010, **86**, 492–498.
37) J. Luo and J. Zhang, *ACS Catal.*, 2016, **6**, 873–877.
38) T.Y. Shang, L. H. Lu, Z. Cao, Y. Liu, W. M. He and B. Yu, *Chem. Commun.*, 2019, **55**, 5408–5419.
39) F. Hundemer, L. Graf von Reventlow, C. Leonhardt, M. Polamo, M. Nieger, S. M. Seifermann, A. Colsmann and S. Bräse, *ChemistryOpen*, 2019, **8**, 1413–1420.
40) M. Yuan, Z. Song, S. O. Badir, G. A. Molander and O. Gutierrez, *J. Am. Chem. Soc.*, 2020, **142**, 7225–7234.
41) (a) Y. Y. Gui, L. Sun, Z. P. Lu and D. G. Yu, *Org. Chem. Front.*, 2016, **3**, 522–526.; (b) J. K. Matsui, S. B. Lang, D. R. Heitz and G. A. Molander, *ACS Catal.*, 2017, **7**, 2563–2575.
42) Á. Gutierrez-Bonet, J. C. Tellis, J. K. Matsui, B. A. Vara and G. A. Molander, *ACS Catal.*, 2016, **6**, 8004–8008.
43) (a) C. Lévêque, L. Chenneberg, V. Corcé, J. P. Goddard, C. Ollivier and L. Fensterbank, *Org. Chem. Front.*, 2016, **3**, 462–465; (b) N. R. Patel, C. B. Kelly, M. Jouffroy and G. A. Molander, *Org. Lett.*, 2016, **18**, 764–767; (c) M. Jouffroy, G. H. M. Davies and G. A. Molander, *Org. Lett.*, 2016, **18**, 1606–1609.; (d) M. Jouffroy, C. B. Kelly and G. A. Molander, *Org. Lett.*, 2016, **18**, 876–879.
44) C. Lévêque, L. Chenneberg, V. Corcé, C. Ollivier and L. Fensterbank, *Chem. Commun.*, 2016, **52**, 9877–9880.
45) J. K. Matsui and G. A. Molander, *Org. Lett.*, 2017, **19**, 436–439.
46) H. Huang, X. Li, C. Yu, Y. Zhang, P. S. Mariano and W. Wang, *Angew. Chem. Int. Ed.*, 2017, **56**, 1500–1505.

47) (a)S. O. Badir, A. Dumoulin, J. K. Matsui and G. A. Molander, *Angew. Chem. Int. Ed.*, 2018, **57**, 6610–6613.; (b) J. Yi, S. O. Badir, L. M. Kammer, M. Ribagorda and G. A. Molander, *Org. Lett.*, 2019, **21**, 3346–3351.
48) D. Madsen, C. Azevedo, I. Micco, L. K. Petersen and N. J. V. Hansen, *Prog. Med. Chem.*, 2020, **59**, 181–249.
49) J. P. Phelan, S. B. Lang, J. Sim, S. Berritt, A. J. Peat, K. Billings, L. Fan and G. A. Molander, *J. Am. Chem. Soc.*, 2019, **141**, 3723–3732.
50) (a) C. H. Basch, J. Liao, J. Xu, J. J. Piane and M. P. Watson, *J. Am. Chem. Soc.*, 2017, **139**, 5313–5316; (b) F. J. R. Klauck, M. J. James and F. Glorius, *Angew. Chem. Int. Ed.*, 2017, **56**, 12336–12339; (c) J. Wu, L. He, A. Noble and V. K. Aggarwal, *J. Am. Chem. Soc.*, 2018, **140**, 10700–10704;(d) F. Sandfort, F. Strieth-Kalthoff, F. J. R. Klauck, M. J. James and F. Glorius, *Chem. Eur. J.*, 2018, **24**, 17210–17214; (e) J. Hu, G. Wang, S. Li and Z. Shi, *Angew. Chem. Int. Ed.*, 2018, **57**, 15227–15231; (f) M. Ociepa, J. Turkowska and D. Gryko, *ACS Catal.*, 2018, **8**, 11362–11367; (g) M. M. Zhang and F. Liu, *Org. Chem. Front.*, 2018, **5**, 3443–3446.; (h) F. J. R. Klauck, H. Yoon, M. J. James, M. Lautens and F. Glorius, *ACS Catal.*, 2019, **9**, 236–241; (i) X. Jiang, M. M. Zhang, W. Xiong, L. Q. Lu and W. J. Xiao, *Angew. Chem. Int. Ed.*, 2019, **58**, 2402–2406; (j) J. Wu, P. S. Grant, X. Li, A. Noble and V. K. Aggarwal, *Angew. Chem. Int. Ed.*, 2019, **58**, 5697–5701.
51) H. G. Roth, N. A. Romero and D. A. Nicewicz, *Synlett*, 2016, **27**, 714–723.
52) Y. Luo, Á. Gutiérrez-Bonet, J. K. Matsui, M. E. Rotella, R. Dykstra, O. Gutierrez and G. A. Molander, *ACS Catal.*, 2019, **9**, 8835–8842.
53) (a) O. Gutierrez, J. C. Tellis, D. N. Primer, G. A. Molander and M. C. Kozlowski, *J. Am. Chem. Soc.*, 2015, **137**, 4896–4899; (b) M. Mohadjer Beromi, G. W. Brudvig, N. Hazari, H. M. C. Lant and B. Q. Mercado, *Angew. Chem. Int. Ed.*, 2019, **131**, 6155–6159; (c) Q. Lin and T. Diao, *J. Am. Chem. Soc.*, 2019, **141**, 17937–17948.
54) T. J. Steiman, J. Liu, A. Mengiste and A. G. Doyle, *J. Am. Chem. Soc.*, 2020, **142**, 7598–7605.
55) M. S. Santos, A. G. Corrêa, M. W. Paixão and B. König, *Adv. Synth. Catal.*, 2020, **362**, 2367–2372.
56) M. Garbacz and S. Stecko, *Adv. Synth. Catal.*, 2020, **362**, 3213–3222.
57) (a) A. Brennführer, H. Neumann and M. Beller, *Angew. Chem. Int. Ed.*, 2009, **48**, 4114–4133; (b) S. Roy, S. Roy and G. W. Gribble, *Tetrahedron*, 2012, **68**, 9867–9923; (c) J. R. Martinelli, T. P. Clark, D.A. Watson, R. H. Munday and S. L. Buchwald, *Angew. Chem. Int. Ed.*, 2007, **119**, 8612–8615; (d) S. D. Friis, T. Skrydstrup and S. L. Buchwald, *Org. Lett.*, 2014, **16**, 4296–4299. For a review on the use of stable CO–surrogates, see: E Serrano and R. Martin, *Eur. J. Org. Chem.* 2018, 3051–3064.
58) N. Alandini, L. Buzzetti, G. Favi, T. Schulte, L. Candish, K. D. Collins and P. Melchiorre, *Angew. Chem. Int. Ed.*, 2020, **59**, 5248–5253.
59) R. S. Mega, V. K. Duong, A. Noble and V. K. Aggarwal, *Angew. Chem. Int. Ed.*, 2020, **59**, 4375–4379.
60) For leading examples: (a) Z. Zuo, H. Cong, W. Li, J. Choi, G. C. Fu and D. W. C. MacMillan, *J. Am. Chem. Soc.*, 2016, **138**, 1832–1835; (b) W. Ding, L. Q. Lu, Q. Q. Zhou, Y. Wei, J. R. Chen and W. J. Xiao, *J. Am. Chem. Soc.*, 2017, **139**, 63–66; (c) H. H. Zhang, J. J. Zhao and S. Yu, *J. Am. Chem. Soc.*, 2018, **140**, 16914–16919.; (d) F. D. Lu, D. Liu, L. Zhu, L. Q. Lu, Q. Yang, Q. Q. Zhou, Y. Wei, Y. Lan and W. J. Xiao, *J. Am. Chem. Soc.*, 2019, **141**, 6167–6172. For a recent review: (e) H. H. Zhang, H. Chen, C. Zhu and S. Yu, *Sci. China Chem.*, 2020, **63**, 637–647; (f) A. Lipp, S. O. Badir and G. A. Molander, *Angew. Chem. Int. Ed.*, 2021, **60**, 1714-1726.
61) H. Pellissier in *Enantioselective Nickel catalyzed transformation*, RSC 2016.
62) E. E. Stache, T. Rovis and A. G. Doyle, *Angew. Chem. Int. Ed.*, 2017, **129**, 3733–3737.
63) H. Guan, Q. Zhang, P. J. Walsh and J. Mao, *Angew. Chem. Int. Ed.*, 2020, **59**, 5172–5177.
64) C. Pezzetta, D. Bonifazi and R. W. M. Davidson, *Org. Lett.*, 2019, **21**, 8957–8961.
65) Q. Y. Meng, S. Wang and B. König, *Angew. Chem. Int. Ed.*, 2017, **129**, 13611–13615.
66) Q. Y. Meng, S. Wang, G. S. Huff and B. Konig, *J. Am. Chem. Soc.*, 2018, **140**, 3198–3201.
67) N. J. Turro, V. Ramamurthy and J. C. Scaiano, in Modern Molecular Photochemistry of Organic Molecules, University Science Books, California, 2010, pp. 629–704.
68) Y. Masuda, N. Ishida and M. Murakami, *Eur. J. Org. Chem.*, 2016, **2016**, 5822–5825.
69) T. E. Schirmer, A. Wimmer, F. W. C. Weinzierl and B. König, *Chem. Commun.*, 2019, **55**, 10796–10799.
70) P. E. Krach, A. Dewanji, T. Yuan and M. Rueping, *Chem. Commun.*, 2020, **56**, 6082–6085.
71) H. Fuse, H. Mitsunuma and M. Kanai, *J. Am. Chem. Soc.*, 2020, **142**, 4493–4499.
72) L. Huang and M. Rueping, *Angew. Chem. Int. Ed.*, 2018, **57,** 10333–10337**.**
73) L. Huang, T. Ji and M. Rueping, *J. Am. Chem. Soc.*, 2020, **142**, 3532–3539.
74) C. Fischer and C. Sparr, *Angew. Chem. Int. Ed.*, 2018, **57**, 2436–2440.
75) Y. Du, R. M. Pearson, C. H. Lim, S. M. Sartor, M. D. Ryan, H. Yang, N. H. Damrauer and G. M. Miyake, *Chem. Eur. J.*, 2017, **23**, 10962–10968.
76) For reviews, see: (a) K. C. Cartwright, A. M. Davies and J. A. Tunge, *Eur. J. Org. Chem.*, 2020, 1245–1258; (b) M. Kojima and S. Matsunaga, *Trends Chem.*, 2020, **2**, 410–426.
77) D. Kalsi, S. Dutta, N. Barsu, M. Rueping and B. Sundararaju, *ACS Catal.*, 2018, **8**, 8115–8120.
78) D. Kalsi, N. Barsu, S. Chakrabarti, P. Dahiya, M. Rueping and B. Sundararaju, *Chem. Commun.*, 2019, **55**, 11626–11629.
79) Q. Y. Meng, T. E. Schirmer, K. Katou and B. König, *Angew. Chem. Int. Ed.*, 2019, **131**, 5723–5728.
80) P. Z. Wang, J. R. Chen and W. J. Xiao, *Org. Biomol. Chem.*, 2019, **17**, 6936–6951.
81) J. C. Grenier-Petel and S. K. Collins, *ACS Catal.*, 2019, **9**, 3213–3218.
82) L. Niu, J. Liu, H. Yi, S. Wang, X. A. Liang, A. K. Singh, C. W. Chiang and A. Lei, *ACS Catal.*, 2017, **7**, 7412–7416.
83) K. C. Cartwright, E. Joseph, C. G. Comadoll and J. A. Tunge, *Chem. Eur. J.*, 2020, **26**, 12454–12471.
84) M. Osawa, H. Nagai and M. Akita, *Dalt. Trans.*, 2007, 827–829.
85) J. Jiang, W. M. Zhang, J. J. Dai, J. Xu and H. J. Xu, *J. Org. Chem.*, 2017, **82**, 3622–3630.
86) C. Zhou, P. Li, X. Zhu and L. Wang, *Org. Lett.*, 2015, **17**, 6198–6201.
87) B. Zhao, R. Shang, W. M. Cheng and Y. Fu, *Org. Chem. Front.*, 2018, **5**, 1782–1786.
88) L. Wang, T. Wang, G. J. Cheng, X. Li, J. J. Wei, B. Guo, C. Zheng, G. Chen, C. Ran and C. Zheng, *ACS Catal.*, 2020, **10**, 7543–7551.
89) E. B. McLean and A. L. Lee, *Tetrahedron*, 2018, **74**, 4881–4902.
90) W. Fu, W. Guo, G. Zou and C. Xu, *J. Fluor. Chem.*, 2012, **140**, 88–94.
91) C. Tian, Q. Wang, X. Wang, G. An and G. Li, *J. Org. Chem.*, 2019, **84**, 14241–14247.
92) X. Chen, Z. Tan, Q. Gui, L. Hu, J. Liu, J. Wu and G. Wang, *Chem. Eur. J.*, 2016, **22**, 6218–6222.
93) R. Jin, Y. Chen, W. Liu, D. Xu, Y. Li, A. Ding and H. Guo, *Chem. Commun.*, 2016, **52**, 9909–9912.

94) A. Tlahuext-Aca, L. Candish, R. A. Garza-Sanchez and F. Glorius, *ACS Catal.*, 2018, **8**, 1715–1719.
95) K. Okada, K. Okamoto and M. Oda, *J. Am. Chem. Soc.*, 1988, **110**, 8736–8738.
96) X. F. Xia, G. W. Zhang, D. Wang and S. L. Zhu, *J. Org. Chem.*, 2017, **82**, 8455–8463.
97) V. T. Nguyen,V. D. Nguyen, G. C. Haug, N. T. H. Vuong, H. T. Dang, H. D. Arman, and O. V. Larionov, *Angew. Chem. Int. Ed.* 2020, **59**, 7921-7927.
98) I. Bauer and H. J. Knölker, *Chem. Rev.*, 2015, **115**, 3170–3387.
99) H. Rao, L. C. Schmidt, J. Bonin and M. Robert, *Nature*, 2017, **548**, 74–77.
100) H. Rao, C. H. Lim, J. Bonin, G. M. Miyake and M. Robert, *J. Am. Chem. Soc.*, 2018, **140**, 17830–17834.
101) M. Neumeier, U. Chakraborty, D. Schaarschmidt, V. de la Pena O'Shea, R. Perez-Ruiz and A. Jacobi von Wangelin, *Angew. Chem. Int. Ed.*, 2020, **59**, 13473–13478.
102) B. Huang, M. Hu and F. D. Toste, *Trends Chem.*, 2020, **2**, 707–720.
103) L. Mei, J. M. Veleta and T. L. Gianetti, *J. Am. Chem. Soc.*, 2020, **142**, 12056–12061.
104) A. Tlahuext-Aca, M. N. Hopkinson, B. Sahoo and F. Glorius, *Chem. Sci.*, 2016, **7**, 89–93.
105) K. S. Egorova and V. P. Ananikov, *Organometallics*, 2017, **36**, 4071–4090.
106) (a) A. Fürstner and N. Shi, *J. Am. Chem. Soc.*, 1996, **118**, 12349–12357; (b) A. Fürstner, *Chem. Rev.*, 1999, **99**, 991–1046.
107) J. L. Schwarz, F. Schäfers, A. Tlahuext-Aca, L. Lückemeier and F. Glorius, *J. Am. Chem. Soc.*, 2018, **140**, 12705–12709.
108) H. Mitsunuma, S. Tanabe, H. Fuse, K. Ohkubo and M. Kanai, *Chem. Sci.*, 2019, **10**, 3459–3465.
109) J. L. Schwarz, H. M. Huang, T. O. Paulisch and F. Glorius, *ACS Catal.*, 2020, **10**, 1621–1627.
110) S. Tanabe, H. Mitsunuma and M. Kanai, *J. Am. Chem. Soc.*, 2020, **142**, 12374–12381.
111) T. McCallum, X. Wu and S. Lin, *J. Org. Chem.*, 2019, **84**, 14369–14380.
112) (a) A. Fürstner and A. Hupperts, *J. Am. Chem. Soc.*, 1995, **117**, 4468–4475; (b) A. Gansäuer, *Chem. Commun.*, 1997, 457–458.
113) Z. Zhang, R. B. Richrath and A. Gansäuer, *ACS Catal.*, 2019, **9**, 3208–3212.
114) S. Lin, Y. Chen, F. Li, C. Shi and L. Shi, *Chem. Sci.*, 2020, **11**, 839–844.
115) A. Gualandi, F. Calogero, M. Mazzarini, S. Guazzi, A. Fermi, G. Bergamini and P. G. Cozzi, *ACS Catal.*, 2020, **10**, 3857–3863.
116) R. E. Estévez, J. Justicia, B. Bazdi, N. Fuentes, M. Paradas, D. Choquesillo-Lazarte, J. M. García-Ruiz, R. Robles, A. Gansäuer, J. M. Cuerva and J. E. Oltra, *Chem. Eur. J.*, 2009, **15**, 2774–2791.
117) (a) M. Wada, K. Akiba K., *Tetrahedron Lett.* 1985, *26*, 4211–4214; (b) M. Wada, H. Ohki, K. Akiba, *Bull. Chem. Soc. Jpn.* 1990, **63**, 1738–1747; (c) N. Miyoshi, M. Nishio, S. Murakami, T. Fukuma, M. Wada *Bull. Chem. Soc. Jpn.* 2000, **73**, 689–692; (d) P. C. Andrews, A. C. Peatt, C. L. Raston, *Green Chem.* 2001, **3**, 313–315; (e) D. Miyamoto, N. Daikawa, K. Tanaka, *Tetrahedron Lett.* 2003, **44**, 6963–6964; (f) K. Smith, S. Lock, G. A. El-Hiti, M. Wada, N. Miyoshi, *Org. Biomol. Chem.* 2004, **2**, 935–938; (g) J. H. Dam, P. Fristrup, R. Madsen*, J. Org. Chem.* 2008, **73**, 3228–3235.
118) (a) M. Wada, H. Ohki, K.-J. Akiba, *J. Chem. Soc., Chem. Commun.* 1987, **10**, 708–709; (b) M. Wada, T. Fukuma, M. Morioka, T. Takahashi, N. Miyoshi, *Tetrahedron Lett.* 1997, **38** 8045–8048; (c) B. D. Jadhav, S. K. Pardeshi, *Tetrahedron Lett.* 2014, **55**, 4948–4952; (d) M. Minato, J. Tsuji, *Chem. Lett.* 1988, **17**, 2049–2052.
119) R. Ping-Da, P. Shi-Feng, D. Ting-Wei and W. Shi-Hui, *Chin. J. Chem.* 1996, **14**, 462-466.
120) S. Potenti, A. Gualandi, A. Puggioli, A. Fermi, G. Bergamini and P. G. Cozzi, *Eur. J. Org. Chem*., 2021, DOI: 10.1002/ejoc.202001640.
121) R. A. Sheldon and J. K. Kochi*, J. Am. Chem. Soc.* 1968, **90**, 6688-6688.
122) A. Hu, J.-J. Guo, H. Pan, H. Tang, Z. Gao, and Z. Zuo, *J. Am. Chem. Soc.* 2018, **140**, 1612−1616.
123) A. Hu, Y. Chen, J.-J. Guo, N. Yu, Q. An, and Z. Zuo, *J. Am. Chem. Soc.* 2018, **140**, 13580−13585.